

University of Twente

Assessing the generalizability of FRAP by comparing results from two confocal microscopes

Fabian de Bree

Bachelor Thesis BMT

Developmental BioEngineering (DBE)

Supervisor: Dr. Ing. J.N. Post

Daily supervisor: Dr. K. Govindaraj

External member: Prof. Dr. Ir. I.M. Vellekoop

June 21

Foreword

Enschede, 28/06/2021

After three years of studying biomedical engineering, the bachelor thesis can be seen as a final proof of competence. It feels exciting to use the academic skills acquired during these years and to focus on a specific problem during a ten-week assignment. Looking back, I can say that those ten weeks flew by and that there was still more that I wanted to do. Because of my interest in cell biology the department of Developmental BioEngineering (DBE) was a logical choice. Another wonderful aspect of a bachelor thesis is the feeling of trying to find answers for a specific problem that can be used in a broader research within the department. At first, the Covid regulations seems to hinder the practical work in the labs. I am more than glad that I was able to perform the practical work myself and to get familiar with different techniques, like FRAP, transfection, and cell culture. Besides the practical work, I have also learned about data processing, analysing smaller problems, and to cope with setbacks. For all of this I would like to thank my supervisor Janine Post, my daily supervisor Kannan Govindaraj, and Ivo Vellekoop as external committee member.

Table of contents

Foreword.....	2
List of Abbreviations.....	4
Summary	5
1. Introduction.....	6
1.1 SOX9-mGFP and BMP7	6
1.2 Fluorescence Recovery After Photobleaching (FRAP)	6
1.3 Confocal microscopy	8
1.4 Goals and hypothesis.....	8
2. Materials and Method.....	9
2.1 Cell culture	9
2.2 Transfection.....	9
2.3 Imaging buffer and coverslips	9
2.4 Fluorescent Recovery After Photobleaching (FRAP).....	10
2.4.1 Determining settings	10
2.4.2 Settings used	10
2.5 FRAP calculations.....	11
3. Results	12
3.1 Cell culture and transfection	12
3.2 FRAP	12
3.2.1 Comparison conditions Zeiss and Nikon.....	13
3.2.2 Effect of using BICor	13
3.2.3 Effect of smaller frame size on SOX9-mGFP recovery curve	16
3.2.4 Comparison calculated FRAP rates MATLAB and Zeiss Zen software	16
4. Discussion.....	18
4.1. Cell culture and transfection	18
4.2 FRAP settings and experiments	18
4.3 FRAP results.....	19
4.4 Data processing.....	20
5. Conclusion	21
6. Recommendations.....	21
Acknowledgements	22
References.....	22
Appendices	23
Appendix A – Dutch Abstract.....	23
Appendix B – Mann-Whitney U test.....	24

Appendix C – Initial intensity (I_0) and intensity loss (IL) in ROI ₂	25
Appendix D – Effect of BICor on FRAP parameters SOX9-mGFP.....	26
Appendix E – Results SOX9-mGFP + IL1 β	27
Appendix F – MATLAB Script	28
Appendix G – Zeiss Protocol.....	34

List of Abbreviations

Abbreviation	Explanation
--------------	-------------

AU	airy unit
(m)GFP	(monomeric) green fluorescent protein
(TF-)FRAP	(transcription factor-) fluorescence recovery after photobleaching
A ₁	Population of fast diffusing proteins
A ₂	Population of slow diffusing proteins
BICor	bleach correction
BMP	bone morphogenetic protein
CLSM	confocal laser scanning microscope
DBE	developmental bioengineering
FCS	fluorescence correlation spectroscopy
FLAP	fluorescence localization after photobleaching
FLIP	fluorescence loss in photobleaching
I_0	initial intensity
IF	immobile fraction
IL	intensity loss
mGFP	monomeric green fluorescent protein
PTHrP	parathyroid hormone-related protein
ROI	region of interest
RT	room temperature
SMM	single-molecule microscopy
SOX9	sex determining region Y box9
STD	standard deviation
TF	transcription factor
TGF- β	transforming growth factor- β
t_{half}	half-time to recovery

Summary

SOX9 is the master transcription factor for cartilage formation. SOX9 is, just like other DNA binding transcription factors, highly mobile when it is not bound to DNA. However, this mobility will decrease when a transcription factor binds to DNA, thereby being able to regulate gene expression. SOX9 activity may be regulated via various pathways and cytokines. For example, BMP7 is an anabolic cytokine that can stimulate cartilage formation and upregulate *SOX9* gene expression, and previous work in the DBE group has shown that BMP7 also regulates SOX9 activity at the protein activity level. In one of those previous studies it has been shown with a Nikon A1 confocal microscope that the changes in SOX9 mobility can be measured with Fluorescence Recovery After Photobleaching (FRAP) and can be related to SOX9 activity. It has also been shown that BMP7 promotes SOX9 activity. However, there are multiple variables that can influence the FRAP results. In this research, C20/A4 cells were treated with BMP7 and the mobility of SOX9 was studied.

The purpose of this study was to compare the results from the Nikon with a Zeiss confocal microscope to study whether FRAP is a generally applicable method for studying protein dynamics, and to develop a protocol for FRAP experiments on the Zeiss microscope.

The results show significant differences between the data obtained on the Zeiss and Nikon microscopes. Based on the Zeiss data, BMP7 has an insignificant inhibiting effect on SOX9. There are also differences between data processing with MATLAB and the Zeiss Zen software. It was expected that the FRAP rates between the Nikon and Zeiss would be similar, but differences in these rates were observed. Other challenges include a relatively low transfection efficiency and changes in the MATLAB scripts. Due to the large number of variables in this study it is inconclusive if FRAP is a generalizable method.

1. Introduction

1.1 SOX9-mGFP and BMP7

Sex determining region Y Box 9 (SOX9) is the master transcriptional regulator for cartilage formation [1]. Binding to DNA transactivates SOX9 target genes, such as *COL2A1* and *ACAN*. The expression of *SOX9* correlates with a high level of *COL2A1* expression in chondrocytes and *SOX9* is present in all chondrogenic progenitors and chondrocytes in articular cartilage [2]. However, *SOX9* expression is not present in the hypertrophic zone of the growth plate. *SOX9* expression is the highest in the resting and proliferating zone [3]. Chondrocyte hypertrophy is inhibited by *SOX9*. *SOX9* is able to inhibit the late stages of chondrogenesis by suppressing cartilage vascularization, and inducing overexpression of parathyroid hormone-related protein (PTHrP), which can inhibit chondrocyte maturation [4]. *SOX9* can also inhibit the expression of matrix degrading proteins like MMP13 [5].

There are multiple signalling pathways that regulate the expression of *SOX9* during chondrogenesis. Transforming Growth Factor- β (TGF- β) is for example able to stabilize *SOX9* by intracellular Smad signalling [5]. Smad can bind to DNA and regulate the expression of *SOX9*. Bone morphogenetic proteins (BMPs) are soluble mediators that belong to the TGF- β superfamily and are involved in the tuning of cellular processes including cell proliferation and differentiation [6]. BMP7 is in cartilage formation an anabolic factor, which means that it can promote cell growth and differentiation. BMP7 can promote chondrogenic extracellular matrix synthesis, increase or maintain the chondrogenic potential and prevent chondrocyte hypertrophy. It has been shown that treatment with BMP7 can increase the mRNA levels of *SOX9* and type 2 collagen [7]. The upregulation of *SOX9* by BMP7 is regulated by intracellular Smad signalling or Smad-independent MAP kinase pathway [8].

A transcription factor (TF), such as *SOX9*, is highly mobile when it is not bound to DNA [9]. However, the mobility decreases when a TF binds to DNA. The relative mobility can be measured and is correlated with the level of activity, making it an interesting parameter for studying the activity of *SOX9* [9].

1.2 Fluorescence Recovery After Photobleaching (FRAP)

Fluorescence Recovery After Photobleaching (FRAP) can be used to study protein dynamics in living cells [10]. To visualize the protein of interest, cells must be transfected with a fluorescent fusion protein. This can be done by linking a fluorescent marker to this protein [11]. Green fluorescent protein (GFP) is a commonly used fluorescent label for FRAP. There are different derivatives of GFP, including monomeric GFP (mGFP).

During FRAP experiments, a high-intensity laser pulse is used to bleach a (circular) region of interest (ROI) [9]. The post-bleaching fluorescence recovery in this region can be measured and plotted against time. A higher mobility will require less imaging time [10]. ROI₁ is used for bleaching, while ROI₂ is a similar sized region placed at a location away from ROI₁ to measure the imaging-induced intensity loss. Correction for this loss is needed, because it can be assumed that this loss is present throughout the whole cell. When this loss is relatively large, the uncorrected recovery curve will show a slight decrease over time. ROI₃ is placed outside the cell and is used to measure the background intensity. The intensity for the recovery curve is normalized to the pre-bleaching intensity by subtracting the background intensity and correcting for the imaging-induced intensity loss as measured in ROI₂.

The recovery is dependent on the mobility of the protein, while the mobility is affected by two major factors: diffusion and chemical interactions [10]. The diffusion constant (*D*) determines the rate of diffusion. Chemical interactions of a protein in a living cell can consist of interactions with other proteins or with DNA/RNA. Transcription factors can for example bind to DNA. The binding and dissociation constants of these interactions will affect the mobility. The principle of FRAP is the same for most proteins, but the fitting of the FRAP curve is dependent on the complex formation and function of the

protein of interest. Therefore, transcription factors need a two-component fit, instead of the general single-component fit.

Proper fitting of the FRAP curve is needed, because not all proteins have these chemical interactions [10]. Untagged mGFP has no intracellular binding site, so the post-bleach intensity will recover almost completely seconds after photobleaching. Therefore, the recovery curve can be fitting with a so-called single-component fit. On the other hand, SOX9 can bind to DNA, so a FRAP curve of SOX9-mGFP needs a different fitting. The recovery will in this case be the result of two factors, namely fast (weak/non-specific binding to DNA) and slow diffusion (strong/specific binding to DNA). A single-component fit is in this case not sufficient, and a two-component fit is needed. Figure 1 shows the fittings of the recovery curves of mGFP and SOX9-mGFP. The equations for the fits will be discussed in section 2.5. In the SOX9-mGFP recovery curve is the present of a shoulder indicated, which reveals that more than one process contributes to the post-bleach recovery. This curve also recovers slower than that of mGFP, and the recovery continues over time due to the exchange at the binding sites.

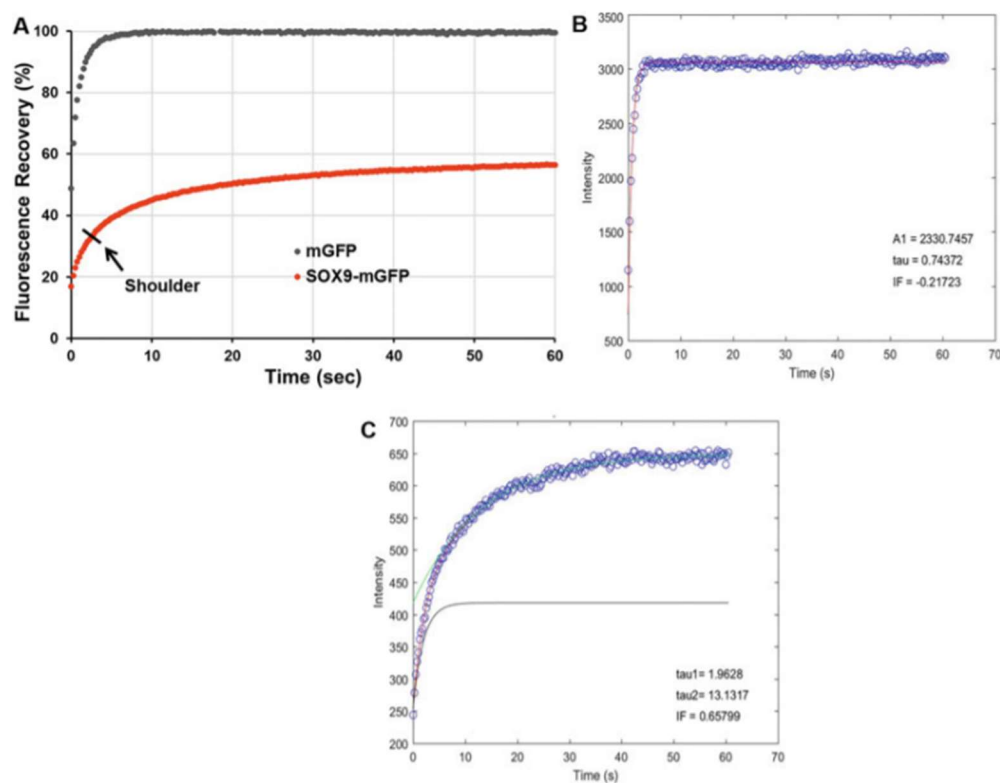


Figure 1 – (A) FRAP curves of mGFP (grey) and SOX9-mGFP (red). The SOX9-mGFP curve contains a shoulder, which is also indicated by the arrow. (B) The fitting of the mGFP curve with a single-component fit. The blue dots are data points, and the red line is the fit. (C) The SOX9-mGFP curve is fitted with a two-component fit. The blue dots are the data points. The grey and green lines are the one- and two-component fits, respectively [10].

A method to gather information on TF dynamics and activity is with the use of Transcription Factor-Fluorescent Recovery After Photobleaching (TF-FRAP), which uses a two-component fit [9]. TF-FRAP uses the principle that TFs bound the DNA are immobile, as is also mentioned above. Changes in DNA binding in response to external stimuli can also be studied with TF-FRAP [9].

Quantitative measures of protein dynamics can be derived from the TF-FRAP data, such as the immobile fraction (IF), half-time to recovery ($t_{1/2}$), and the ratio of the fast diffusing population (A_1 , unbound) to slow diffusing population (A_2 , interaction with binding site) (A_1/A_2) of the fluorescent fractions [9]. The IF indicates the fraction of proteins that is bound to DNA, and thus immobile, and therefore will not

contribute to the recovery of post-bleaching intensity. At the same time these molecules occupy binding sites for incoming unbleached proteins [10]. The t_{half1} of A_1 and t_{half2} of A_2 indicates half the time required for the fast and slow diffusing populations to recover, respectively. A typical TF-FRAP curve fitting with a two-component fit can be seen in Figure 2, together with indicated parameters.

There are also other techniques besides FRAP that can be used for visualizing and studying protein mobility. Single-Molecule Microscopy (SMM) is a method where a fluorescently labelled protein can be tracked, allowing visualization of immobile proteins [12]. Drawbacks of this method include the requirement of specialized equipment and the chance of imaging-induced photobleaching. Fluorescence Correlation Spectroscopy (FCS) can be used to study protein diffusion and kinetics but mostly require instruments that are limited available in comparison with FRAP equipment. Fluorescence loss in photobleaching (FLIP) and fluorescence localization after photobleaching (FLAP) are techniques that are comparable with FRAP [13]. FLIP provides insight in protein kinetics by measuring the decline in intensity in a ROI after repetitive photobleaching. FLAP uses two fluorescent tags: one for bleaching and the other as reference for tracking. An advantage is that those methods require similar protocols and instruments as with FRAP. A drawback is that these techniques are sensitive to imaging-induced loss of fluorescence.

1.3 Confocal microscopy

Confocal microscopes have generally a higher axial resolution as compared to traditional widefield microscopes due to the presence of two pinholes which suppress the detection of out-of-focus light [14]. Most light is blocked by the pinhole. The diameter of the pinhole can be changed, thereby also changing the amount of light that can pass through. The diameter of the pinhole is two times the minimal lateral resolution and is referred to as 1 Airy Unit (AU). A coherent laser beam is used for excitation. This light, together with fluorescent light emitted from the specimen, passes through a dichroic mirror, thereby splitting the light based on wavelength differences. A confocal laser scanning microscope (CLSM) scans the specimen and measures the intensity [15]. This measured intensity is used for the recovery curve.

1.4 Goals and hypothesis

A study performed by Govindaraj et al. [9] has shown that FRAP can be used for studying SOX9-mGFP mobility. However, there are relatively few comparable studies performed with similar conditions but a different microscope. It is therefore not completely known if FRAP is a solid method and if the results will be the same when using a different microscope, settings, or when the experiments are executed

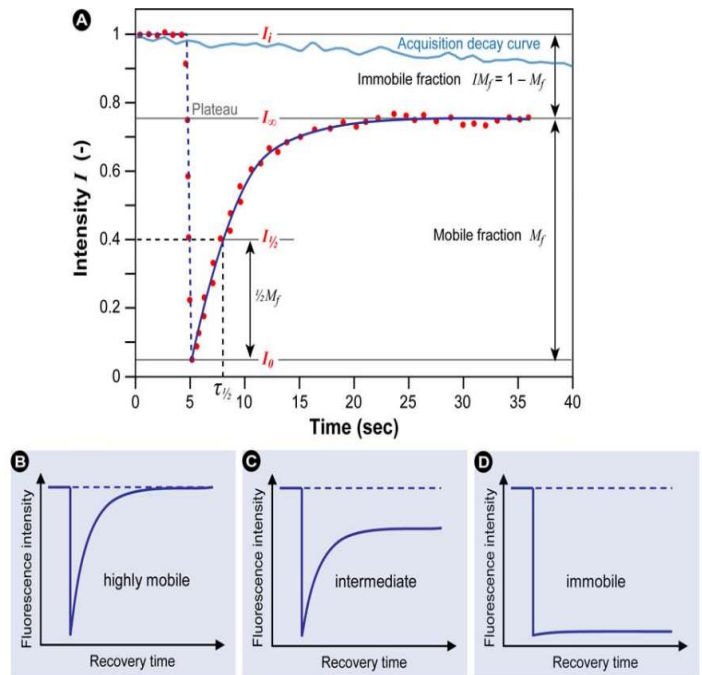


Figure 2 – Typical TF-FRAP curve. (A) The red dots are the data points, and the blue line is the fit. The initial, pre-bleach, intensity (I_i) starts at 1 and drops to a lower value (I_0) after bleaching in the ROI. Ideally, the fluorescence will gradually recover to an intensity that will not increase any further in time (I_∞). The half-recovery time ($t_{1/2}$) with the corresponding intensity ($I_{1/2}$) are also indicated, just as the mobile and immobile fractions. The light blue graph shows the reference curve of fluorescence loss inside ROI₂ during data collection. The recovery can be related to the mobility, and thus activity, of the protein of interest. This can either be (B) highly mobile, (C) intermediate mobile with an immobile fraction, or (D) immobile [13].

by another researcher. In this research, similar conditions were used as the previously mentioned study, together with the same cell line: immortalized human chondrocytes (C20/A4). The main difference is that a Nikon A1 CLSM was used by Govindaraj et al., while in this study a Zeiss LSM 880 CLSM was used.

The purpose of this research is to study whether FRAP experiments performed on a Zeiss LSM 880 CLSM can provide similar results as a Nikon A1 CLSM, and thereby proves to be a solid method for studying protein dynamics, and to conduct a protocol for FRAP experiments with the Zeiss microscope.

The hypothesis is that treatment with BMP7 will increase SOX9-DNA binding and thereby its mobility will decrease. SOX9-mGFP will have a higher IF than mGFP, but smaller than the treatment with BMP7. The curve will have a similar shape with a plateau, so parameters such as the IF will be comparable between the microscopes and the overall effect of BMP7 on SOX9 mobility will most likely also be similar. Exact values will probably differ between the two microscopes since there are a lot of variables in the experiments, and the experience of the researcher can also influence the results, but the data should be useable for relative comparison with the same trend in conditions.

2. Materials and Method

2.1 Cell culture

The human chondrocyte cell line C20/A4 was used [16]. These cells are derived from juvenile costal chondrocytes and are immortalized. C20/A4 cells with passage numbers 23-26 were used. Complete media consisted of DMEM (Gibco), 10% FBS (Gibco) and 1% penicillin-streptomycin (Gibco). Incubation was done at 37°C with 5% CO₂ and this was used for all incubation, unless otherwise mentioned. Cells were initially cultured in a T25 flask (Greiner Bio-One) and transferred to larger flasks when the confluency was 90-100%.

2.2 Transfection

Cells were cultured in 24 well plate (VWR) on glass coverslips (Ø12mm) at least one day prior to the transfection at a density of 40.000 cells/well. The confluence for the transfections was between 70-80%. Lipofectamine LTX and Plus Reagent (Invitrogen) was used for transfection, with both types of plasmids: mGFP (pCMV6, Origene) and SOX9-mGFP (pCMV6, Origene). Both plasmids had a concentration of 1 ng/µl. A transfection mix was made for 2 wells, with mix A consisting of 50 µl OptiMEM (Gibco) and 2 µl Lipofectamine LTX and mix B consisting of 50 µl OptiMEM, 1 µl DNA and 1 µl Plus Reagent. After 5 minutes of incubation at room temperature (RT), the mixes were added together, forming the final transfection mix. The final mix was incubated for 5 minutes at RT. The cells were washed once with OptiMEM. After that, 200 µl OptiMEM and 50 µl transfection mix was added. The plate was incubated for 1.5 h. After this time, OptiMEM and the mix are replaced with complete medium after washing once with DMEM. The efficiency of the transfection was observed one day after the transfection with an EVOS M5000 (Invitrogen) with GFP filter.

2.3 Imaging buffer and coverslips

24 h after transfection, one coverslip was used for imaging. The cells were washed once with imaging buffer. The imaging buffer was composed of 135 mM NaCl (Sigma), 10 mM KCl (Sigma) 0.4 mM MgCl₂ (Sigma), 1 mM CaCl₂ (Sigma), 10 mM HEPES (Acros organics), pH adjusted to 7.2, filter sterilized and stored at -20 °C [9]. On the day of imaging, 250 µl glucose and 50 µl BSA was freshly added. For imaging, a silicon holder on a glass slide was filled with imaging buffer and the coverslip was placed on top with the cells facing down. In this way, an airtight environment was created. The cells were subsequently transported to the microscope for FRAP measurements. For the condition with BMP7, BMP7 was added directly to the imaging buffer in the setup with a final concentration of 100 ng/ml. FRAP was performed after 2.5 h of incubation at 37°C with 5% CO₂ with BMP7.

2.4 Fluorescent Recovery After Photobleaching (FRAP)

The first step was to get familiar with the microscope and determine optimal settings that can be used for all FRAP experiments. These settings were saved in the Zeiss Zen software.

2.4.1 Determining settings

Fixated C20/A4 cells transfected with SOX9-mGFP (1 ng/ μ l, pCMV6, Origene) were used to determine the settings for the FRAP experiments. The intensity in the ROI bleached will not recover because the cells are fixed. The shape and intensity of the bleaching spot can therefore be studied. When the intensity of the laser is too high for imaging or bleaching the cells can suffer from phototoxicity, which can also affect the results [17]. The pinhole was set to 1 AU (\varnothing 60 μ m) as a starting point for the other settings. The zoom was changed until the frame covers only one entire nucleus. The frame size of 256x256 pixels and the ROI size of 3.16 μ m was similar as used by Govindaraj et al. [9]. The scan speed was set to maximal to have the fastest imaging possible.

The gain was based on the intensity of a handful of cells and the range indicator was used to check for saturated pixels. The offset determines the minimal intensity detected by the sensor. The value for the offset was set to have enough fluorescent signal in the nucleus while having an as low as possible intensity in the background. The laser intensity for imaging was set as low as possible to avoid imaging-induced bleaching. The laser intensity and iterations for bleaching were determined by trial and error. The bleaching spot should have a shape similar to the ROI chosen and the intensity should decrease visible. One iteration was preferred, to have a more direct effect and the fastest imaging after bleaching. The scan speed is indicated with a number but does not represent the number of frames per second. Different combinations of scan speed (SS) and laser intensity (I) were used. The results are shown in Figure 3. This data shows that an increase in scan speed requires a higher bleaching intensity. The fluorophore used was kind of hard to bleach, and in combination with the scan speed set to maximum it was difficult to get a good bleach spot. Therefore, the highest laser intensity was used for bleaching.

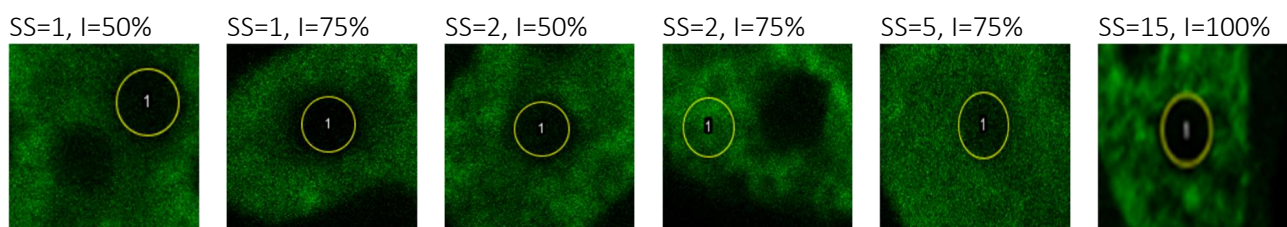


Figure 3 - Bleaching results for different settings of the scan speed (SS) and laser intensity (I) used for bleaching. All images were taken with fixated C20/A4 cells transfected with SOX9-mGFP. The image of scan speed 15 and 100% laser intensity is taken from a living C20/A4 cell but is shown as there is no data from the fixed cells with the same settings.

2.4.2 Settings used

FRAP measurements were performed with a Zeiss LSM 880 Airyscan confocal microscope (Carl Zeiss AG) with a 63x water immersion objective. For each condition, FRAP was performed on 40 cells during one session of 3 h. Cells were only used if the fluorescence intensity was average in comparison with the other cells and if the nucleus had a normal shape. Examples of used cells are shown in Figure 4. The pixel saturation was checked with the software when in doubt. The gain was set to 700 and was constant for all measurements. The frame size was 256x256 pixels and covered the entire nucleus. A single pixel was 0.1054 μ m, so the imaged area had a size of 27x27 μ m. A zoom of 5.0 and a pinhole size of 1 AU (\varnothing 60 μ m) was used.

Bleaching was done with a 488 nm laser at 100% power for 1 iteration. The bleached area (ROI₁) consisted of a circular region with a diameter of 3.16 μ m (30 pixels) in a region where the fluorescence

intensity was representative for the overall intensity in the cell measured. Two similar sized regions were chosen: one inside the nucleus, other than the region bleached, for reference (ROI₂), and one outside the nucleus for background intensity (ROI₃). The scan time was 130.25 msec (7.7 FPS), which was the maximum scan speed (15) with these settings.

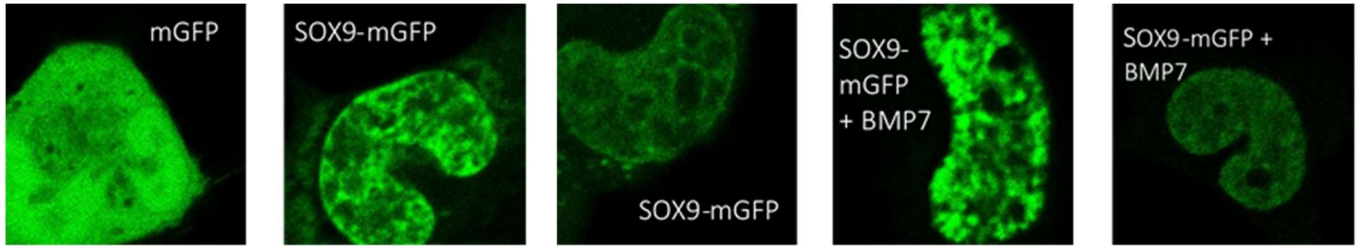


Figure 4 – Examples of the C20/A4 cells used for FRAP experiments for all of the conditions.

For each measurement, twenty-five pre-bleaching imaging were taken. The fluorescence intensity of the last ten pre-bleach images was averaged and used for normalizing the post-bleach data. The post-bleaching scanning time consisted of 425 images, or approximately 60 s. FRAP data was saved as .txt files and analysed using a previous established MATLAB™ script (Mathworks; R2019b, Appendix F). A protocol for FRAP measurements can also be found in Appendix G. Some data was also saved from the Zeiss Zen software to make a comparison with the data from MATLAB.

FRAP data from SOX9-mGFP was provided by a E.S. Meima (June 2021), using same methods for cell culture, transfection, and FRAP measurements.

2.5 FRAP calculations

The data was fitted to equations in MATLAB (Mathworks; R2019b) [10]. mGFP has no binding site and the mobility of mGFP can thus be described with a single-component fit:

$$F(t) = y_0 + A_1 \left(1 - e^{-\frac{t}{\tau_1}} \right) \quad (1)$$

where y_0 corresponds to the fluorescent intensity at the first post-bleach frame, A_1 to the fraction of fast (unbound) diffusing proteins, and τ_1 is the recovery time constant for the fast population. The half-time to recovery was calculated using equation (2):

$$t_{half1} = \ln(2) * \tau_1 \quad (2)$$

For SOX9-mGFP and SOX9-mGFP with BMP7 this was a two-component fit:

$$F(t) = y_0 + A_1 \left(1 - e^{-\frac{t}{\tau_1}} \right) + A_2 \left(1 - e^{-\frac{t}{\tau_2}} \right) \quad (3)$$

In equation (3) y_0 corresponds to the fluorescent intensity at the first post-bleach frame and is automatically calculated by MATLAB, A_1 to the fraction of fast (unbound) diffusing proteins, A_2 to the fraction of slow (bound) diffusing proteins, and τ_1 and τ_2 are the recovery time constants for the fast and slow population, respectively.

The immobile fraction (IF), was calculated using equation (4):

$$IF = I_0 - I_E \quad (4)$$

where I_0 is the initial intensity and I_E is the intensity in the last frame of the recovery curve.

The half-time to recovery of the fast and slow populations, t_{half1} and t_{half2} , were calculated using equation (2), only with either τ_1 or τ_2 , respectively. All values for the parameters of both fits are determined or calculated by MATLAB.

3. Results

3.1 Cell culture and transfection

Approximately 40.000 C20/A4 cells (p23-26) were cultured 24h prior to transfection. Figure 5A shows how the cells looked prior to the transfection and 24 h after seeding, where the confluency is approximately 60%. The average confluency 24 h after transfection was 70-80%, as is shown in Figure 5B and 5C. The blurry cells are caused by the presence of cells under the coverslip, thereby being out of focus. The efficiency was overall relatively low ($\pm 5\%$) and was even lower in parts with higher confluency. This efficiency is lower than preferred and limit the number of cells to use for the FRAP experiments.

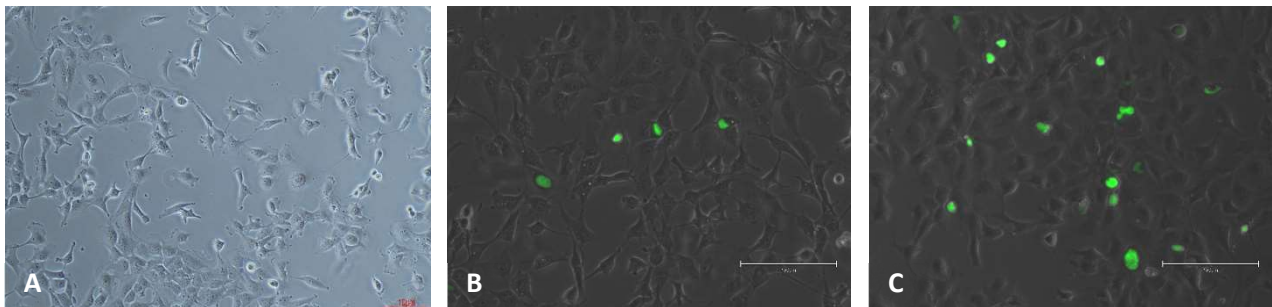


Figure 5 – C20/A4 cells before and after transfection. (A) C20/A4 cells seeded on coverslips prior to transfection with SOX9-mGFP (Nikon Eclipse TS100; 10x). Scale bar = 10 μm . Both (B) and (C) show the cells 24 h after transfection but were taken of different coverslips with different transfection efficiencies (EVOS M5000; 20x). Scale bar = 150 μm .

3.2 FRAP

In Figure 6, images are shown of one bleached nucleus per condition, including the corresponding ROI's. The data from the conditions was compared between the Zeiss and Nikon microscopes. Also the influence of bleach correction (BICor) on the recovery curves and FRAP parameters was observed. For SOX9-mGFP also a frame size of 128x128 pixels was used instead of 256x256 pixels. The calculated parameters are also compared for all conditions between the used MATLAB script and the Zeiss Zen software, which is the software used for operating the microscope and data acquisition.

Table 1 – Calculated average values of FRAP parameters (\pm standard deviation) for all conditions with both the Zeiss and Nikon CLSM.

Condition	t_{half1} (s)	t_{half2} (s)	IF (%)	A_1/A_2
mGFP Zeiss	$1,02 \pm 0,56$	-	$0,21 \pm 0,09$	-
mGFP Nikon	$1,39 \pm 0,91$	-	$0,12 \pm 0,08$	-
SOX9-mGFP Zeiss (128x128 pixels)	$0,99 \pm 0,54$	$11,00 \pm 7,87$	$24,4 \pm 10,1$	$1,27 \pm 0,85$
SOX9-mGFP Zeiss	$1,84 \pm 0,56$	$15,10 \pm 6,10$	$37,0 \pm 9,0$	$1,05 \pm 0,47$
SOX9-mGFP Nikon	$1,48 \pm 0,31$	$13,83 \pm 5,52$	$53,7 \pm 5,0$	$0,84 \pm 0,25$
SOX9-mGFP + BMP7 Zeiss	$1,39 \pm 0,57$	$13,67 \pm 8,60$	$36,1 \pm 10,8$	$1,02 \pm 0,47$
SOX9-mGFP + BMP7 Nikon	$2,43 \pm 0,62$	$19,48 \pm 5,66$	$66,8 \pm 4,3$	$0,55 \pm 0,25$

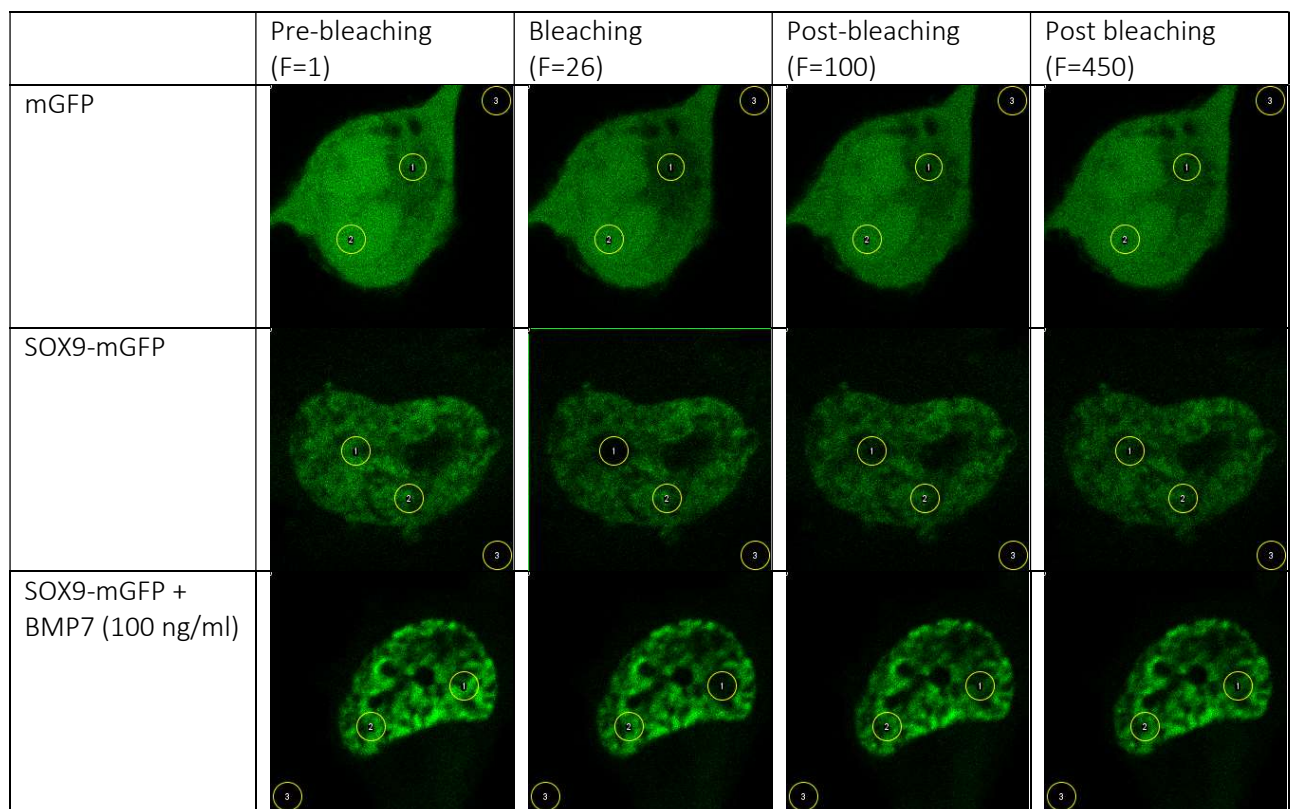


Figure 6 – Images of one bleached nucleus per condition. The frame (F) of the image is indicated for the four images: pre-bleached (F=1), bleaching (F=26), post-bleaching (F=100) and (F=450). The total number of frames was 450 for each condition.

3.2.1 Comparison conditions Zeiss and Nikon

The recovery curves for mGFP, SOX9-mGFP, and SOX9-mGFP + BMP7 are shown in Figure 7A for both the Zeiss and Nikon microscope. The recovery curves of mGFP are for both microscopes quite similar, with a recovery of almost 100%. The recovery curves from SOX9-mGFP and SOX9-mGFP + BMP7 lie higher than the same conditions from the Nikon data. Figure 7C-F and Table 1 show the values for the FRAP parameters for each condition calculated for both microscopes. Not only are the absolute values between the microscopes different, but also the trend within the conditions is different. For example, BMP7 seems to have an inhibiting effect on SOX9 mobility, which can be seen from the higher recovery curve and the slightly lower IF. Mann-Whitney U tests are used to determine statistical significance between conditions or between the microscopes (Appendix B). t_{half1} was significantly different between SOX9-mGFP and SOX9-mGFP + BMP7 on the Zeiss. All FRAP parameters for BMP7 are significantly different between the Zeiss and the Nikon. For SOX9-mGFP this is limited to t_{half1} and IF. Figure 7B also shows the recovery curve of SOX9-mGFP + Il1 β for both microscopes. Il1 β seems to have an inhibiting effect on SOX9 mobility. This data was adapted from the bachelor thesis of E.S. Meima (June 2021), who used the same protocols, and is used as an extra comparison. More published data for this condition is shown in Appendix E.

3.2.2 Effect of using BICor

BICor can influence the calculated FRAP parameters and the recovery curves. This effect is investigated by comparing the same data but with and without the use of BICor. The influence of BICor on the recovery curves can be seen in Figure 8. The curve for mGFP gets a different shape when not using BICor and the recovery is lower than with BICor. The recovery curves of SOX9-mGFP and SOX9-mGFP + BMP7 have a higher final recovery when using BICor but seems to lie parallel to each other, indicating that the effect of BICor is comparable for both conditions. This means that relative comparison is possible. Because the recovery curve changes, the calculated FRAP parameters will also be different.

This is for the parameters of SOX9-mGFP shown in Appendix D. Because there will be differences between, and within, conditions when using BICor, it is advisable to only compare data with the same usage of BICor.

For this research, all data processing was done with the use of BICor, unless otherwise indicated. This choice is based on the percentual intensity loss (IL) in the reference ROI: ROI₂. If the loss in this ROI is relatively large, it can be assumed that this imaging-induced intensity loss is present throughout the whole cell and that therefore BICor should be used. For the calculation of the IL, the initial intensity (I_0 , at frame 16) in the same ROI was used. The I_0 can also provide insight in the intensities of the cells used and whether or not the IL has a correlation with I_0 . This correlation is investigated for every condition by looking at a linear trend line and the corresponding coefficient of determination: R^2 . The average IL and I_0 are for every condition shown in Table 2.

The average I_0 was for the Zeiss microscope for all conditions at least ten times higher. There is also a relatively large spread in I_0 for the conditions imaged with the Zeiss microscope. The spread between the conditions was on the other hand relatively small. The IL was for the Zeiss also higher than for the Nikon, but with a lower standard deviation (STD). Based on the values for R^2 there seems to be no significant correlation between I_0 and IL for both the Zeiss and Nikon microscopes. Because the IL is relatively large, BICor is used for data processing for both the Zeiss and Nikon microscopes. Another reason was that the recovery curve of mGFP seems to be more in line with what is expected when using BICor.

Table 2 – The average (AVG) initial intensity (I_0) and intensity loss (IL) including the standard deviations (STD) for all conditions on both the Zeiss and Nikon microscope. Also, the coefficient of determination (R^2) is indicated between I_0 and IL.

Condition	AVG Initial Intensity (I_0)	STD (I_0)	AVG Intensity Loss (IL) %	STD (IL)	R^2
mGFP Zeiss	26335,8	13162,6	-16,0	2,66	0,0361
mGFP Nikon	2632,63	320,730	-6,4	2,45	0,0060
SOX9 Zeiss	23970,4	8511,33	-18,1	4,98	0,0036
SOX9 Nikon	1524,55	388,833	-7,9	3,66	0,0124
SOX9 + BMP7 Zeiss	22366,6	10207,7	-14,2	5,14	0,0405
SOX9 + BMP7 Nikon	1506,39	363,231	-6,4	1,87	0,0065

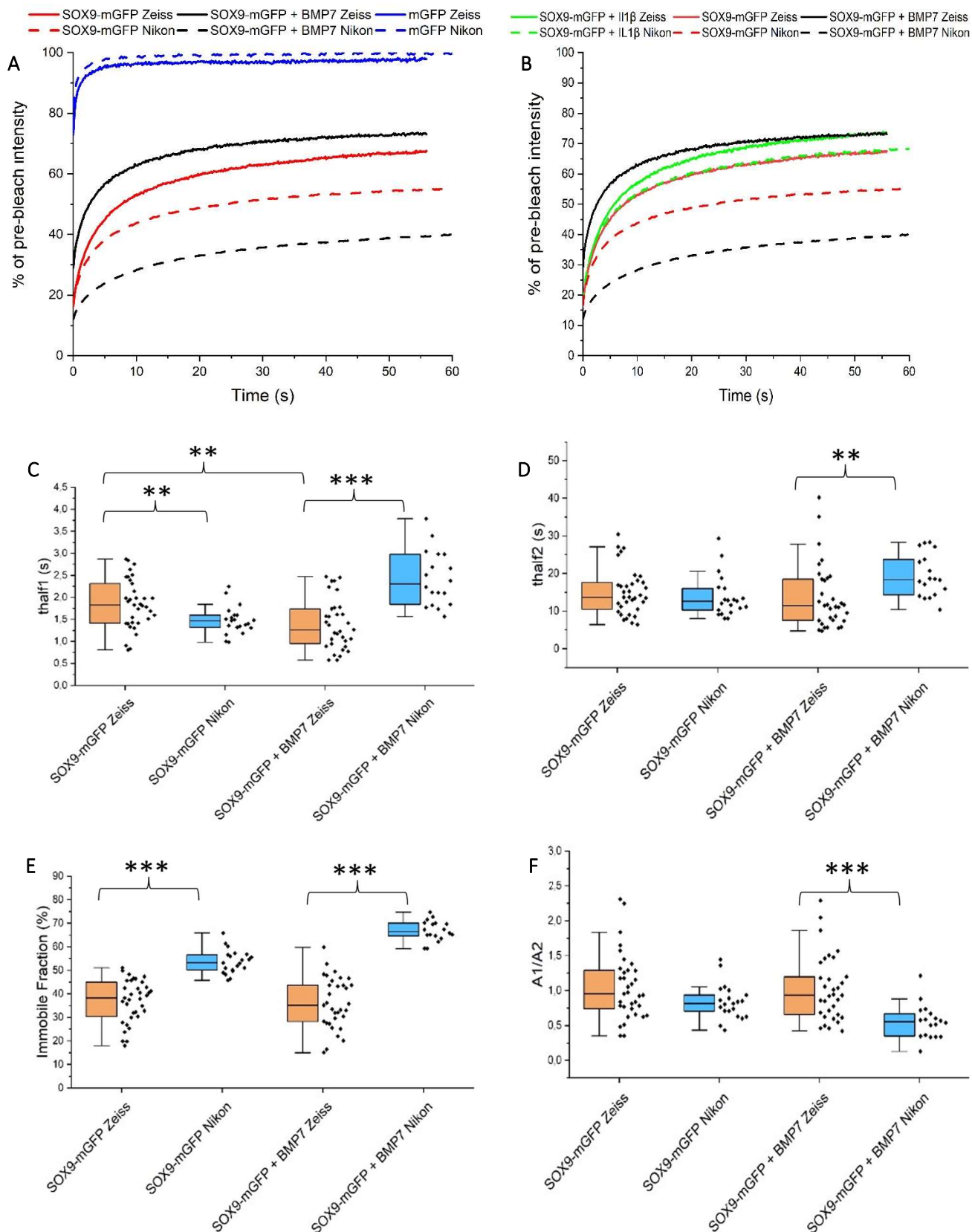


Figure 7 – (A) Recovery curves of all condition on both the Zeiss and the Nikon CLSM. The data from the Zeiss is per condition indicated with a solid line while the corresponding Nikon data is shown with a dashed line. (B) Recovery curves as in (A) but also with the condition SOX9-mGFP + IL1 β (see also Appendix E). (C-F) Boxplots for the FRAP parameters t_{half1} (C), t_{half2} (D), IF (E), and A_1/A_2 (F). All values are indicated for the conditions SOX9-mGFP and SOX9-mGFP + BMP7 for both the Zeiss and Nikon CLSM. Statistical significance was determined with Mann-Whitney U tests and is indicated as follows: * $p < 0.05$, ** $p < 0.01$ *** $p < 0.001$ (See appendix B).

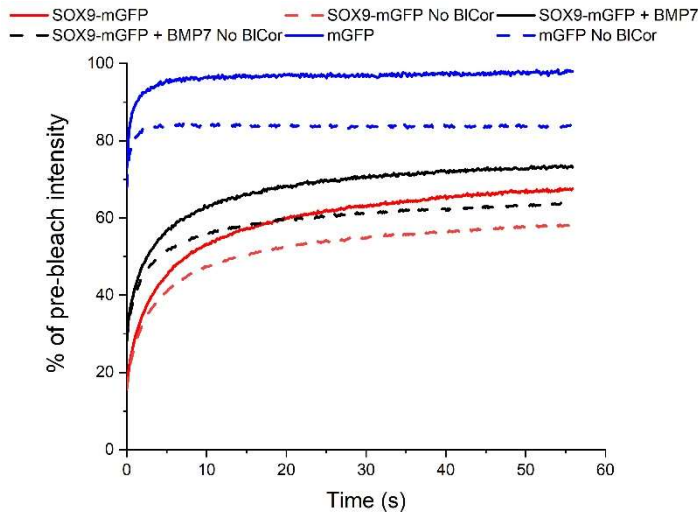


Figure 8 – Influence of bleach correction (BICor) on the recovery curves of the different conditions. The curves with BICor are per condition shown as solid lines, while the curves without BICor are shown as dashed lines. The effects of BICor on the parameters are shown for SOX9-mGFP in Appendix D.

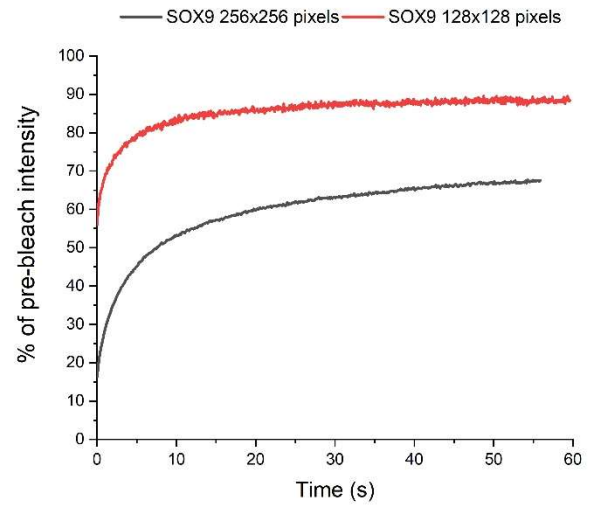


Figure 9 – FRAP recovery curves of SOX9-mGFP for a frame size of 128x128 pixels and 256x256 pixels.

3.2.3 Effect of smaller frame size on SOX9-mGFP recovery curve

For all conditions, a frame size of 256x256 pixels was used. To see how a different frame size could influence the recovery curve, a frame size of 128x128 pixels was used for SOX9-mGFP. The recovery curve is shown in Figure 9. It is visible that the bleaching is less deep, and that the recovery curve has also a different shape with a higher recovery. The values of the FRAP parameters for the lower and normal frame size are also shown in Table 1. Especially t_{half1} is different for both frame sizes, which can also be explained by the different shape of the curves. Based on the visible differences between the data within one condition, comparison of conditions should only be done when using the same frame size.

3.2.4 Comparison calculated FRAP rates MATLAB and Zeiss Zen software

The calculated FRAP parameters for the Zeiss data were compared between the MATLAB script and the Zeiss Zen software. For mGFP this is shown in Figure 10, and for SOX9-mGFP and SOX9-mGFP + BMP7 this is shown in Figure 11. The Zen software allows the user to choose between both the single- and two-component fits, which are the same as described in section 2.5.

The values for t_{half1} are for mGFP quite similar and the Mann-Whitney U test showed no significant differences between the methods of data processing. However, all the IFs showed relatively large differences. Especially the IFs calculated by the Zen software differ greatly from the other two methods, even though the single-component fit was selected in the Zen software.

In contract, the IFs for SOX9-mGFP and SOX9-mGFP + BMP7 are similar, while the other parameters differ at least between one of the conditions. It is also noticeable that the spread in calculated IFs are quite large for both the Zen software and MATLAB. All of the values for t_{half1} , t_{half2} , and A_1/A_2 are, for an unknown reason, higher calculated by the Zen software in comparison with the values from MATLAB, and the differences are for all values and conditions significant between Zen and MATLAB. The differences can be caused by other calculations for y_0 , or the normalization to the pre-bleach intensity.

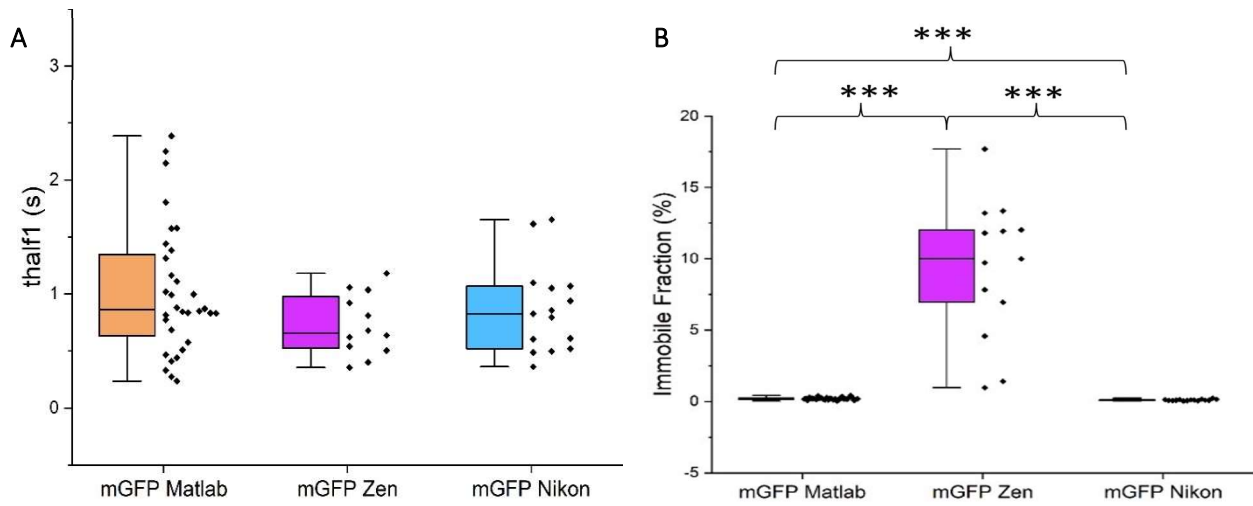


Figure 10 – Boxplots of the FRAP parameters t_{half1} (A) and IF (B) for mGFP. The Zeiss data is shown as calculated by MATLAB (orange) or the Zeiss Zen software (purple). The Nikon data is shown in blue. Statistical significance was determined with Mann-Whitney U tests and is indicated as follows: * $p < 0.05$, ** $p < 0.01$ *** $p < 0.001$ (See appendix B).

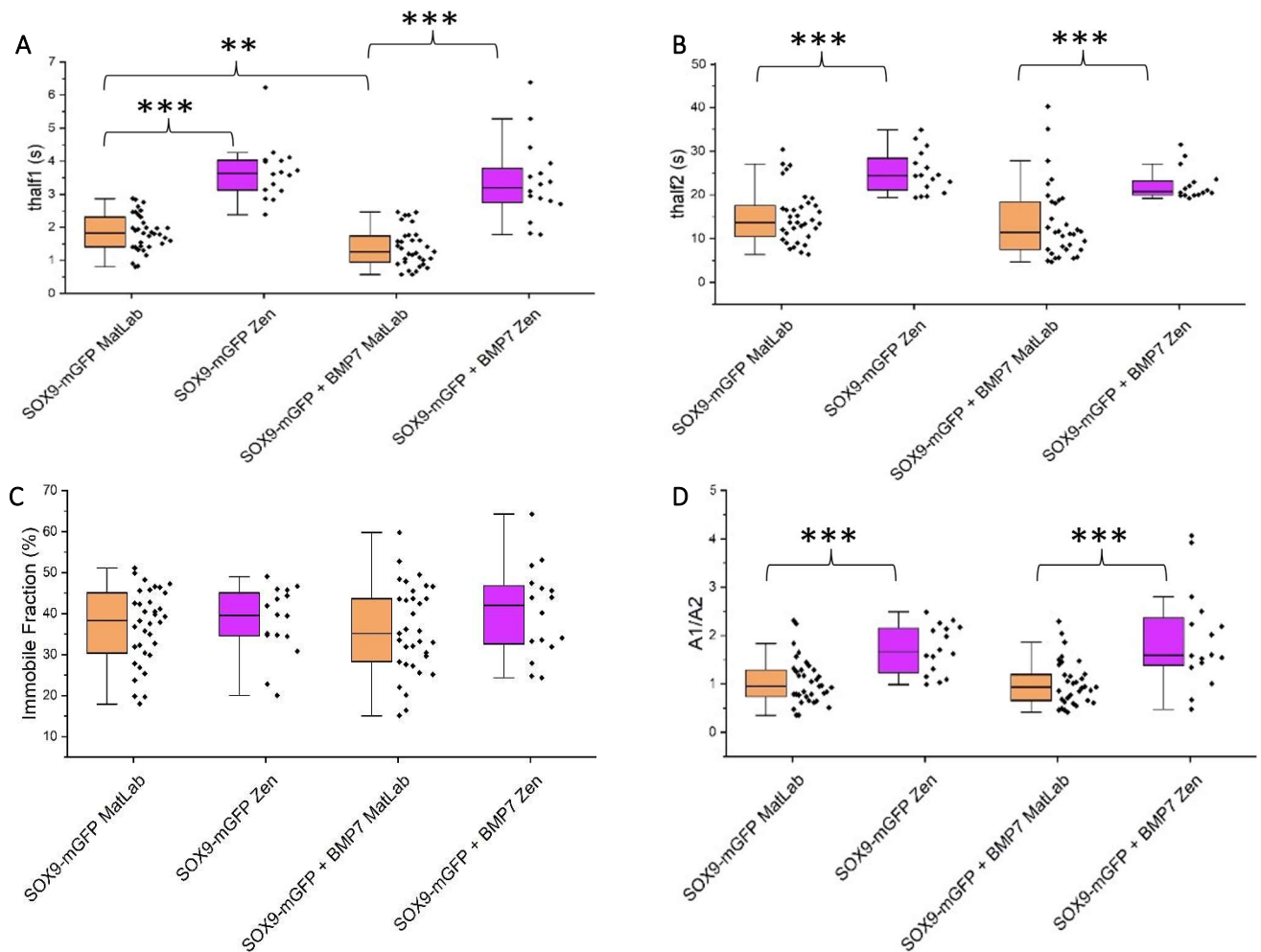


Figure 11 – Boxplots of the FRAP parameters t_{half1} (A), t_{half2} (B), IF (C), and $A1/A2$ (D) for the conditions SOX9-mGFP and SOX9-mGFP + BMP7 calculated by MATLAB (orange) or the Zeiss Zen software (purple). Statistical significance was determined with Mann-Whitney U tests and is indicated as follows: * $p < 0.05$, ** $p < 0.01$ *** $p < 0.001$ (See appendix B).

4. Discussion

One goal of this research was to study whether results on the Zeiss LSM 880 CLSM would be comparable with results previously gathered with a Nikon A1 CLSM. Comparable results would indicate that FRAP is a solid technique for studying protein dynamics. Another goal was to establish a protocol for future FRAP experiments. For doing so, FRAP was performed on C20/A4 cells with the following conditions: mGFP, SOX9-mGFP and SOX9-mGFP + BMP7 (100 ng/ml).

Previous obtained data from the Nikon was used in this research. For a more optimal and reliable comparison the same researcher should perform FRAP experiments on both microscopes because this can also decrease the inter-observer variability. Also the experience of the researcher can have an influence on the results. Beside this, there are a lot of variables in this research that could influence the results.

4.1. Cell culture and transfection

The confluency was not the same for each condition and sometimes differs between coverslips from one condition. The main reason for this is that the time between seeding cells on coverslips and transfection was not the same for each condition. A higher confluency negatively influences the transfection efficiency. The transfection efficiency was checked with a fluorescence microscope. The overall efficiency of $\pm 5\%$ was relatively low. On the website of the manufacturer it is also mentioned that the optimal number of seeded cells differ for cell types, but that generally a confluency of 70-90% at the time of transfection should provide good results [18]. It is advisable to strive for comparable confluency between conditions, for example by seeding different densities or using the same amount of time between seeding and transfection for all conditions.

4.2 FRAP settings and experiments

The gain used has now been determined by looking at a couple of different cells and checking whether the used gain was sufficient. The range-indicator was used to check for saturated pixels. However, a better approach would be to use the intensity histogram and adjust the gain so that there are no under- or oversaturated pixels.

There are a lot of variations between the two microscopes. For example, the diameter of the pinhole is for 1 AU on the Zeiss different from that on the Nikon. Both microscopes also have different detectors. Therefore, the gain and offset do not have to be the same for both microscopes. A relatively large spectrum was used for the detector. In the future, only a smaller spectrum around the peak emission wavelength of mGFP can be used, for example by using a similar spectrum as the GFP Alexa Fluor 488 filter, which has a peak wavelength at 510 nm and a bandwidth of 42 nm [19]. This can help increase the contrast and is better when using more than one fluorophore.

The frame size was changed from 256x256 pixels to 128x128 pixels to study the effect of this change on the recovery curve within the same condition. For the lower frame size, only 25 cells were imaged, and 20 files were used for data processing. This number of cells should be sufficient, but since all conditions show relatively large variations more cells can be imaged to make a more reliable comparison. A lower frame size and faster scanning speed causes the SOX9-mGFP recovery curve to be higher and leads to different values of the FRAP parameters. The change in height can be caused by the less deep bleaching, which indicates that optimization of the settings is needed when using a 128x128 pixels frame size. The resolution is lower, and the bleaching spot was not as round for the lower frame size, thereby possibly influencing the effective bleaching radius.

Although an effort has been made to minimize the differences in fluorescence intensity and appearance of the cells, during the data processing it emerged that relatively large variations were still present. The

average initial intensity is visible in Appendix C. The variation in intensity is relatively high for the Zeiss and it is advisable to use cells with similar intensity. However, it can be difficult to indicate the exact intensity when imaging. The high intensity on the Zeiss can be caused by the highly sensitive gallium arsenide phosphide (GaAsP) detector. The removal of data from cells with intensity lower than 10.000 and higher than 40.000 did, besides from the average intensity, not result in any significant differences in the final data. There was also no clear correlation between I_0 and IF.

During imaging it was sometimes quite difficult to find 40 healthy cells that were similar in both shape and intensity because of the low transfection efficiency. When the efficiency is lower, the signal-to-noise ratio is lower, and the observer is forced to choose among the limit number of cells to image. The cells are heterogenous and this will increase when the number of transfected cells is low, causing a great variety among the imaged cells. Due to time constraints each condition could only be imaged once. For this reason, also some of the less suitable cells were imaged and included in the data set. It is recommended for future experiments to either improve the transfection efficiency so that the number of suitable cells increases or repeat each condition and image each time a lower number of cells, i.e. two times 20 cells. The duration of the imaging session (3h) was also too long for the cells to be out of the incubator and in the imaging buffer. It is better to have multiple cover slips prepared and image each cover slip for about 30 min.

4.3 FRAP results

mGFP was used as a control for both microscopes. The recovery curves of mGFP have a similar shape on both microscopes, which is also what was expected. The C20/A4 cells were incubated with BMP7 to study the changes in the mobility of SOX9. Based on the data from the Nikon it appears that BMP7 decreases SOX9-mGFP mobility (lower recovery curve) and increases the IF. Several experiments were performed on the Nikon A1 CLSM with the same concentration of BMP7 where the results were comparable with the Nikon data used in this research. Those results are in line with what is expected from the pathway of BMP7. However, the Zeiss data shows an opposite effect. The SOX9-mGFP + BMP7 curve lies above that of SOX9-mGFP and the IF of SOX9-mGFP + BMP7 is also somewhat smaller than that of SOX9-mGFP only, indicating that BMP7 has a slightly inhibiting effect. This also contradicts the hypothesis.

The SOX9-mGFP and SOX9-mGFP + BMP7 recovery curves from the Zeiss lie above the same curves from the Nikon. The Zeiss recovery curves are closer to each other than the Nikon curves. The results of the Mann-Whitney U tests show that there is no statistically significant difference between SOX9-mGFP and SOX9-mGFP + BMP7 based on the Zeiss data. Because it is highly unlikely that BMP7 has an inhibiting effect on SOX9-mGFP, the condition should be redone. Moreover, the curve has a shape that is more in line with a BMP7 concentration of 10 ng/ml instead of 100 ng/ml, which can indicate that the dilution was not performed properly [10]. It is also possible that the tube of BMP7 did contain another cytokine or was too old to be used. An ELISA kit can be used to detect BMP7 and validate the content of the tube [20]. Even if the tube contained BMP7, the cytokine could still be biologically inactive. This biological activity could have been checked by using a cell line transfected with BMP-responsive elements of the Id1 promotor fused with a luciferase reporter gene [21]. Biologically active BMPs will induce luciferase expression, which can then be measured with a luminometer.

A part of the differences in data can also be the result of different incubation times and should be considered when comparing data. In this study, the cells were incubated for 2.5 h. In previous research, the cells were incubated with BMP7 (100 ng/ml) for only 1 h under similar incubation conditions [9][10]. In another study, where a different cell line was used, the incubation time for BMP7 was also 1 h [22]. It was advised to incubate for about 2 h to increase the effect of BMP7. The BMP7 was also directly added to the imaging buffer before incubation and imaging. However, the cells may not survive such a long time in the imaging buffer. This can result in less active or dead cells during imaging. In future

research, also the concentration of BMP7 can be varied to see whether this can influence the overall effect on SOX9 mobility with the same incubation time.

In future studies, qPCR can be used to provide insight in the changes in gene expression. This information can be used as extra validation in studying the effect of BMP7 on SOX9 expression. Moreover, the binding of TFs to DNA does not always result in target gene expression because TFs often need co-factors, which may not be present or bound [23].

IL1 β is a negative regulator of cartilage homeostasis and should increase the mobility of SOX9, or decrease the IF [9]. It is visible that the differences in recovery curves for the condition with SOX9-mGFP + IL1 β are larger for the Nikon than for the Zeiss. The recovery curve of IL1 β (Nikon) is almost similar to SOX9-mGFP (Zeiss). The differences between the calculated FRAP parameters for SOX9-mGFP in comparison with the addition of IL1 β proves to be insignificant for the Zeiss. Even the IFs between IL1 β and BMP7 are not significantly different. This indicates that also a condition with a negative cytokine did not give conclusive results.

The low efficacy of BMP7 and IL1 β on SOX9 mobility can also be caused by dedifferentiation of the used cells. Human articular chondrocytes can dedifferentiate with every passage when cultured in monolayer [24]. Moreover, SOX9 expression will decrease quickly in the isolated chondrocytes cultured in monolayer. The manufacturer of the cell line indicates that the cells can be cultured for at least 10 passages without significantly influencing the marker expression and functionality [16]. Because in this study passage numbers 23-26 were used the possibility of dedifferentiation should be considered.

4.4 Data processing

ROI₂ is used for reference to measure the imaging-induced bleaching. The recovery curve should be corrected for this general intensity loss over time, which can be done with the use of bleach correction. 25 pre-bleach images were used from which the last ten are averaged and used as pre-bleach intensity. This number is the same for the Nikon and the Zeiss. However, the Zeiss has roughly twice the frame rate of the Nikon, causing the same number of images to be taken in approximately half the time. When analysing the raw FRAP data it appears that the pre-bleach intensity was still decreasing and did not stabilize when bleaching occurred. This could influence the results because the pre-bleach intensity decrease was less stabilized than the Nikon data. This can partly explain the differences between the Nikon and Zeiss but did not influence the relative comparison of the Zeiss conditions when this decrease in pre-bleach intensity is similar for all conditions. It is important for future experiments to optimize the time, and thus the number of images, needed pre-bleach in order for the intensity decrease to stabilize. Using only the last three pre-bleach images for normalization instead of ten did not influence the results.

In Appendix C is indicated what the IL's are for all conditions on both the Zeiss and Nikon. From the values for R^2 becomes clear that the average bleaching loss is independent of the initial intensity and is roughly similar for the cells measured. The IL's is higher for every condition on the Zeiss and therefore BICor was used.

BICor has an effect on the recovery curves. The changes in data when using BICor can be quite large, as is the clearest for mGFP. BICor does also shift the recovery curves of SOX9-mGFP and SOX9-mGFP + BMP7. However, the use of BICor does not influence the overall effect of BMP7 on SOX9 mobility because the changes due to the use of BICor are quite similar. In Appendix D is shown what the influence is of BICor on the FRAP parameters of SOX9-mGFP. Because the parameters and curves can change, it is highly recommended to only compare data with the similar use of BICor.

Only a single-component MATLAB script was used for processing mGFP data. mGFP is not bound to a protein and has, in contrast to SOX9-mGFP, no binding site. It can therefore diffuse freely through the whole cell. In this case there will be no slow diffusing proteins, so A_2 will be zero. Because the whole cell has a fluorescent signal, the location of the nucleus should be estimated during FRAP experiments. An important point is to make sure that the bleaching ROI is not (partly) in the cytoplasm because otherwise the whole cell will become darker when bleaching.

The calculated FRAP parameters from the Zeiss data are also compared between the used MATLAB script and the Zeiss Zen software. These results show that the t_{half1} values are comparable and that the Zen software has the lowest spread in these values. For the IFs this is totally different: the Nikon and Zeiss (MATLAB) show comparable values, while the IFs calculated with the Zen software are multiple times higher. The differences between the MATLAB calculated values and the Zen software are significant for SOX9-mGFP and SOX9-mGFP + BMP7, except for the IFs. It is notable that both MATLAB and the Zen software have a relatively large spread in calculated IF values. The differences in the other parameters should be considered when acquiring and using data. Further optimization of the MATLAB script is needed to improve the fittings and also be more generally useable, e.g. when using other cells or another microscope. Future data analysis can also be improved by looking at violin plots instead of boxplots to study whether different clusters of cells are present.

A1start and A2start have been changed in the MATLAB script (Appendix F, line 186) in order to improve the fitting of the FRAP curves. The initial values for A1start and A2start were 300 and, respectively. The new values have been determined by creating a for-loop and increasing the values in the same initial ratio until the calculated parameters, such as the IF, did not change anymore for all of the conditions. The higher values can be the result of the higher intensities used in comparison with the Nikon data. It is advisable to improve the MATLAB script in a way that no additional manual adjustments are needed, independent of the data used. This way, also the data processing is more general applicable and independent of the data set and changes made by the user, resulting in more reliable comparisons.

5. Conclusion

There are multiple differences present between the microscopes in both the calculated FRAP parameters and the recovery curves. Due to the large number of variables in the experiments it remains inconclusive if FRAP is a generalizable method for studying protein mobility. Factors like the transfection efficiency, BMP7 effectiveness and concentration, incubation time, detector used, number of cells seeded and imaged, observer, and method of data processing can all influence the results.

6. Recommendations

In future research, it is advisable to:

- Increase the transfection efficiency;
- Incubate with BMP7 before creating an imaging setup;
- Use a smaller spectrum for detector;
- Image for a shorter duration per session;
- Check which cytokine is added and the biological activity;
- Vary the final BMP7 concentration and incubation times;
- Use qPCR as an extra validation to measure the changes in gene expression;
- Improve the data processing in MATLAB so the calculations are more comparable with the Zen software, and no additional manual adjustments in the MATLAB script are needed;
- Redo the experiments on both microscopes by the same researcher;
- Only compare data with the same frame size, scan speed and BICor have been used.

Acknowledgements

This bachelor assignment was executed in the DBE group at the University of Twente. I would like to specially thank Janine Post for the supervision and the opportunity to do this assignment. I also want to thank Kannan Govindaraj as my daily supervisor for the introduction and supervision in the lab, provision of materials, feedback, and knowledge. Also my gratitude for the committee: Janine Post, Kannan Govindaraj, and Ivo Vellekoop. I would also like to thank the whole DBE group, BioNanoLab, SLT, and supervisors in the lab for the use of labs and equipment. I would like to thank Tom Knop and Ine Segers for the possibility of using the Zeiss confocal microscope. Furthermore, I would like to thank Lisa Meima for the collaboration, data sharing and insightful discussions.

References

- [1] Song H, Park KH. Regulation and function of SOX9 during cartilage development and regeneration. *Semin Cancer Biol* 2020;67:12–23. doi:10.1016/j.semcancer.2020.04.008.
- [2] Zhao Q, Eberspaecher H, Lefebvre V, de Crombrughe B. Parallel expression of Sox9 and Col2a1 in cells undergoing chondrogenesis. *Dev Dyn* 1997;209:377–86. doi:10.1002/(SICI)1097-0177(199708)209:4<377::AID-AJA5>3.0.CO;2-F.
- [3] Welting TJM, Karperien M, Post JN. NKX3.2 plays a key role in regulating HIF1 α -directed angiogenesis in chondrocytes. *Biotarget* 2018;2:11–11. doi:10.21037/biotarget.2018.07.01.
- [4] Nishimura R, Hata K, Matsubara T, Wakabayashi M, Yoneda T. Regulation of bone and cartilage development by network between BMP signalling and transcription factors. *J Biochem* 2012;151:247–54. doi:10.1093/jb/mvs004.
- [5] Coricor G, Serra R. TGF- β regulates phosphorylation and stabilization of Sox9 protein in chondrocytes through p38 and Smad dependent mechanisms. *Sci Rep* 2016;6:1–11. doi:10.1038/srep38616.
- [6] Caron MMJ, Emans PJ, Cremers A, Surtel DAM, Coolsen MME, van Rhijn LW, Welting TJM. Hypertrophic differentiation during chondrogenic differentiation of progenitor cells is stimulated by BMP-2 but suppressed by BMP-7. *Osteoarthritis Cartil* 2013;21:604–13. doi:10.1016/j.joca.2013.01.009.
- [7] Shintani N, Hunziker EB. Chondrogenic differentiation of bovine synovium: Bone morphogenetic proteins 2 and 7 and transforming growth factor β 1 induce the formation of different types of cartilaginous tissue. *Arthritis Rheum* 2007;56:1869–79. doi:10.1002/art.22701.
- [8] Zhang L, Luo Q, Shu Y, Zeng Z, Huang B, Feng Y, Zhang B, Wang X, Lei Y, Ye Z, Zhao L, Cao D, Yang L, Chen X, Liu B, Wagstaff W, Reid RR, ... Kang Q. Transcriptomic landscape regulated by the 14 types of bone morphogenetic proteins (BMPs) in lineage commitment and differentiation of mesenchymal stem cells (MSCs). *Genes Dis* 2019;6:258–75. doi:10.1016/j.gendis.2019.03.008.
- [9] Govindaraj K, Hendriks J, Lidke DS, Karperien M, Post JN. Changes in Fluorescence Recovery After Photobleaching (FRAP) as an indicator of SOX9 transcription factor activity. *Biochim Biophys Acta - Gene Regul Mech* 2019;1862:107–17. doi:10.1016/j.bbagr.2018.11.001.
- [10] Govindaraj K, Post JN. Using frap to quantify changes in transcription factor dynamics after cell stimulation: Cell culture, frap, data analysis, and visualization. *Methods Mol. Biol.*, vol. 2221, Humana Press Inc.; 2021, p. 109–39. doi:10.1007/978-1-0716-0989-7_9.
- [11] Lippincott-Schwartz J, Snapp EL, Phair RD. The Development and Enhancement of FRAP as a Key Tool for Investigating Protein Dynamics. *Biophys J* 2018;115:1146–55. doi:10.1016/j.bpj.2018.08.007.
- [12] Fritzsche M, Charras G. Dissecting protein reaction dynamics in living cells by fluorescence recovery after photobleaching. *Nat Protoc* 2015;10:660–80. doi:10.1038/nprot.2015.042.
- [13] Ishikawa-Ankerhold HC, Ankerhold R, Drummen GPC. Advanced fluorescence microscopy techniques-FRAP, FLIP, FLAP, FRET and FLIM. *Molecules* 2012;17:4047–132. doi:10.3390/molecules17044047.
- [14] Naredi-Rainer N, Prescher J, Hartschuh A, Lamb DC. Confocal Microscopy. *Fluoresc. Microsc. From Princ. to Biol. Appl.* Second Ed., Wiley-VCH Verlag; 2017, p. 165–202. doi:10.1002/9783527687732.ch5.
- [15] Braeckmans K, Remaut K, Vandenbroucke RE, Lucas B, De Smedt SC, Demeester J. Line FRAP with the confocal laser scanning microscope for diffusion measurements in small regions of 3-D samples. *Biophys J* 2007;92:2172–83. doi:10.1529/biophysj.106.099838.
- [16] Sigma-Aldrich. C20A4 Human Chondrocyte Cell Line n.d. <https://www.sigmaaldrich.com/catalog/product/mm/scc041> (accessed April 28, 2021).
- [17] Icha J, Weber M, Waters JC, Norden C. Phototoxicity in live fluorescence microscopy, and how to avoid it; Phototoxicity in live fluorescence microscopy, and how to avoid it n.d. doi:10.1002/bies.201700003.
- [18] Thermo Fisher. Factors Influencing Transfection Efficiency n.d. <https://www.thermofisher.com/nl/en/home/references/gibco-cell-culture-basics/transfection-basics/factors-influencing-transfection-efficiency.html> (accessed June 2, 2021).
- [19] Thermo Fisher. Fluorescence SpectraViewer n.d. <https://www.thermofisher.com/order/fluorescence-spectraviewer#!/> (accessed June 16, 2021).
- [20] BioSciences. BMP7 ELISA Kit n.d. https://www.biocompare.com/25138-Assay-Kit/8609769-Human-BMP7-ELISA-Kit-Sandwich-ELISA/?pda=9956%7C8609769_0_1%7C%7C1%7CBMP7&dfp=true (accessed June 22, 2021).
- [21] Zilberberg L, ten Dijke P, Sakai LY, Rifkin DB. A rapid and sensitive bioassay to measure bone morphogenetic protein activity. *BMC Cell Biol* 2007;8:1–10. doi:10.1186/1471-2121-8-41.
- [22] Luo DD, Phillips A, Fraser D. Bone morphogenetic protein-7 inhibits proximal tubular epithelial cell Smad3 signaling via increased SnO expression. *Am J Pathol* 2010;176:1139–47. doi:10.2353/ajpath.2010.090459.
- [23] Spivakov M. Spurious transcription factor binding: Non-functional or genetically redundant? *BioEssays* 2014;36:798–806. doi:10.1002/bies.201400036.
- [24] Tew SR, Clegg PD, Brew CJ, Redmond CM, Hardingham TE. SOX9 transduction of a human chondrocytic cell line identifies novel genes regulated in primary human chondrocytes and in osteoarthritis. *Arthritis Res Ther* 2007;9:R107. doi:10.1186/ar2311.

Appendices

Appendix A – Dutch Abstract

SOX9 is de belangrijkste transcriptiefactor in de formatie van kraakbeen. SOX9 is, net als andere transcriptiefactoren die in staat zijn om aan het DNA te binden, mobiel wanneer het niet gebonden is aan DNA. Echter neemt deze mobiliteit af wanneer een transcriptiefactor aan het DNA bindt en op deze manier in staat is om genexpressie te reguleren. SOX9 activiteit wordt mogelijk op diverse manieren gereguleerd, vooral door zogenaamde *pathways* en cytokines. BMP7 is bijvoorbeeld een anabole cytokine dat in staat is om kraakbeenformatie te stimuleren en *SOX9* gen expressie te verhogen, en uit eerder werk van de DBE vakgroep is gebleken dat BMP7 ook SOX9 op eiwitniveau reguleert. In een van deze eerdere onderzoeken is ook met behulp van een Nikon A1 confocaal microscoop aangetoond dat veranderingen in SOX9 mobiliteit kunnen worden gemeten met *Fluorescence Recovery After Photobleaching* (FRAP) en deze veranderingen kunnen worden gerelateerd aan SOX9 activiteit. Daarnaast is ook aangetoond dat BMP7 een bevorderend effect heeft op SOX9 activiteit. Echter zijn er een divers aantal variabelen die van invloed zijn op de resultaten van FRAP experimenten. In dit onderzoek worden C20/A4 cellen behandeld met BMP7 en wordt de mobiliteit van SOX9 onderzocht. Het doel van dit onderzoek is om resultaten van de Nikon te vergelijken met een Zeiss confocaal microscoop om te onderzoeken of FRAP een algemeen toepasbare methode is om eiwitdynamiek te bestuderen, en om een protocol op te stellen voor FRAP experimenten met de Zeiss microscoop. De resultaten laten zien dat er significante verschillen zijn tussen de data verkregen van de Zeiss en de Nikon microscopen. Op basis van de Zeiss data heeft BMP7 een insignificant remmend effect op SOX9. Er zijn ook verschillen tussen data verwerking met MATLAB en met de Zeiss Zen software. De verwachting was dat de FRAP parameters vergelijkbaar zouden zijn tussen de Nikon en de Zeiss, maar er werden verschillen in deze waarden waargenomen. Andere uitdagingen omvatten onder meer veranderingen in de MATLAB scripts en een relatief lage transfectie efficiëntie. Vanwege de grote hoeveelheid aan variabelen in het onderzoek is het niet met doorslag te zeggen of FRAP een generaliseerbare methode is.

Appendix B – Mann-Whitney U test

Table 3 – Results of the Mann-Whitney U tests performed. Only when the results differ statistically significant this was indicated as follows: * $p < 0.05$, ** $p < 0.01$ *** $p < 0.001$.

P1	P2	Significance
t_{half1} SOX9-mGFP Zeiss MATLAB	t_{half1} SOX9-mGFP Nikon MATLAB	**
t_{half2} SOX9-mGFP Zeiss MATLAB	t_{half2} SOX9-mGFP Nikon MATLAB	
IF SOX9-mGFP Zeiss MATLAB	IF SOX9-mGFP Nikon MATLAB	***
A ₁ /A ₂ SOX9-mGFP Zeiss MATLAB	A ₁ /A ₂ SOX9-mGFP Nikon MATLAB	
t_{half1} BMP7 Zeiss MATLAB	t_{half1} BMP7 Nikon MATLAB	***
t_{half2} BMP7 Zeiss MATLAB	t_{half2} BMP7 Nikon MATLAB	**
IF BMP7 Zeiss MATLAB	IF BMP7 Nikon MATLAB	***
A ₁ /A ₂ BMP7 Zeiss MATLAB	A ₁ /A ₂ BMP7 Nikon MATLAB	***
t_{half1} SOX9-mGFP Zeiss MATLAB	t_{half1} BMP7 Zeiss MATLAB	**
t_{half2} SOX9-mGFP Zeiss MATLAB	t_{half2} BMP7 Zeiss MATLAB	
IF SOX9-mGFP Zeiss MATLAB	IF BMP7 Zeiss MATLAB	
A ₁ /A ₂ SOX9-mGFP Zeiss MATLAB	A ₁ /A ₂ BMP7 Zeiss MATLAB	
t_{half1} SOX9-mGFP Zen	t_{half1} BMP7 Zen	
t_{half2} SOX9-mGFP Zen	t_{half2} BMP7 Zen	
IF SOX9-mGFP Zen	IF BMP7 Zen	
A ₁ /A ₂ SOX9-mGFP Zen	A ₁ /A ₂ BMP7 Zen	
t_{half1} SOX9-mGFP MATLAB	t_{half1} SOX9-mGFP Zen	***
t_{half2} SOX9-mGFP MATLAB	t_{half2} SOX9-mGFP Zen	***
IF SOX9-mGFP MATLAB	IF SOX9-mGFP Zen	
A ₁ /A ₂ SOX9-mGFP MATLAB	A ₁ /A ₂ SOX9-mGFP Zen	***
t_{half1} BMP7 MATLAB	t_{half1} BMP7 Zen	***
t_{half2} BMP7 MATLAB	t_{half2} BMP7 Zen	***
IF BMP7 MATLAB	IF BMP7 Zen	
A ₁ /A ₂ BMP7 MATLAB	A ₁ /A ₂ BMP7 Zen	***
t_{half1} mGFP MATLAB	t_{half1} mGFP Zen	
t_{half1} mGFP MATLAB	t_{half1} mGFP Nikon	
t_{half1} mGFP Nikon	t_{half1} mGFP Zen	
IF mGFP MATLAB	IF mGFP Zen	***
IF mGFP MATLAB	IF mGFP Nikon	***
IF mGFP Nikon	IF mGFP Zen	***

Appendix C – Initial intensity (I_0) and intensity loss (IL) in ROI₂

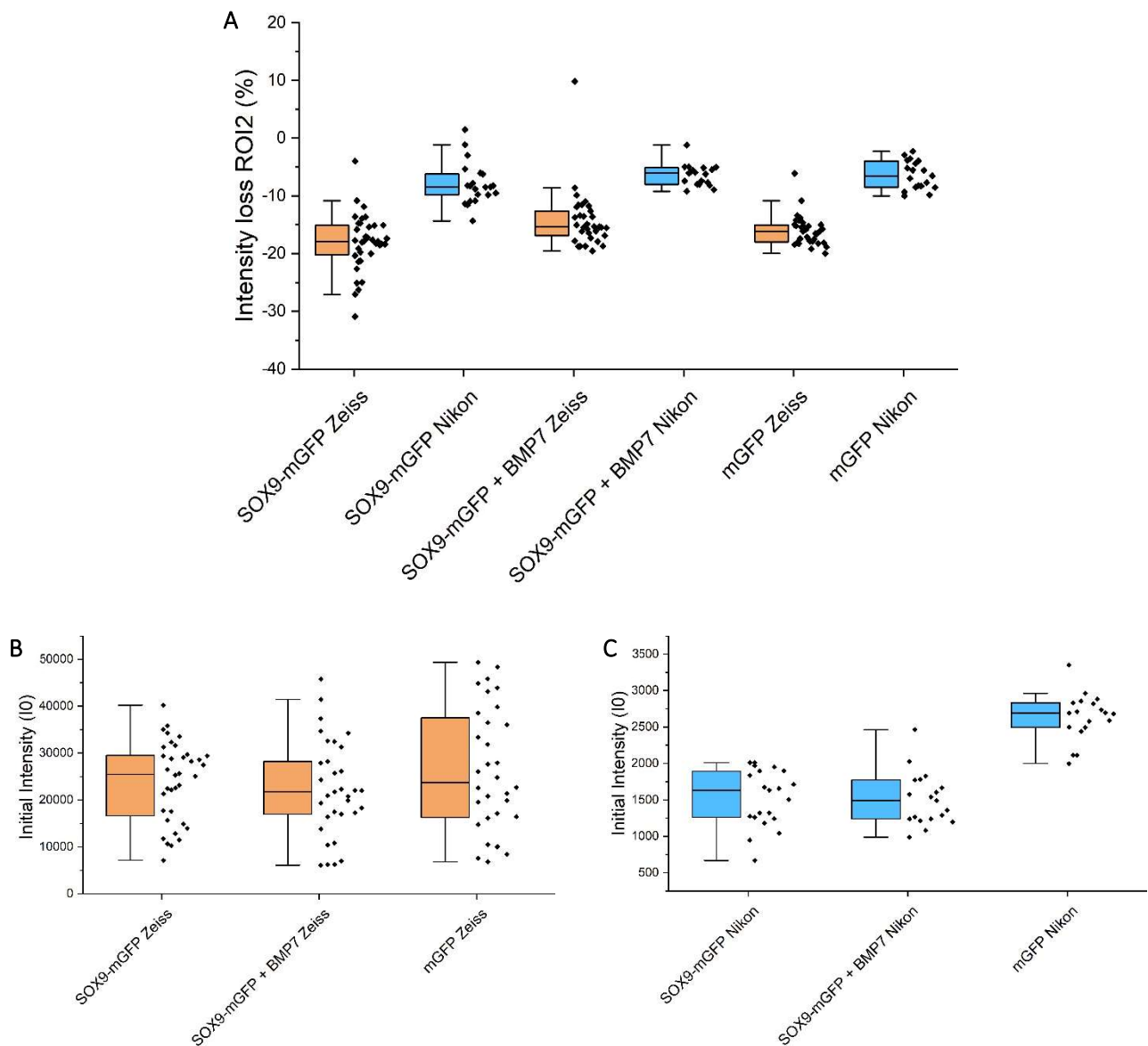


Figure 12 – (A) Boxplot of the percentual intensity loss (IL) in ROI₂ as calculated between I_0 (frame 16) and the last time frame (frame 450). (B-C) Boxplots of the initial intensity (I_0) of all the cells used for the Zeiss (B) and the Nikon (C).

Appendix D – Effect of BICor on FRAP parameters SOX9-mGFP

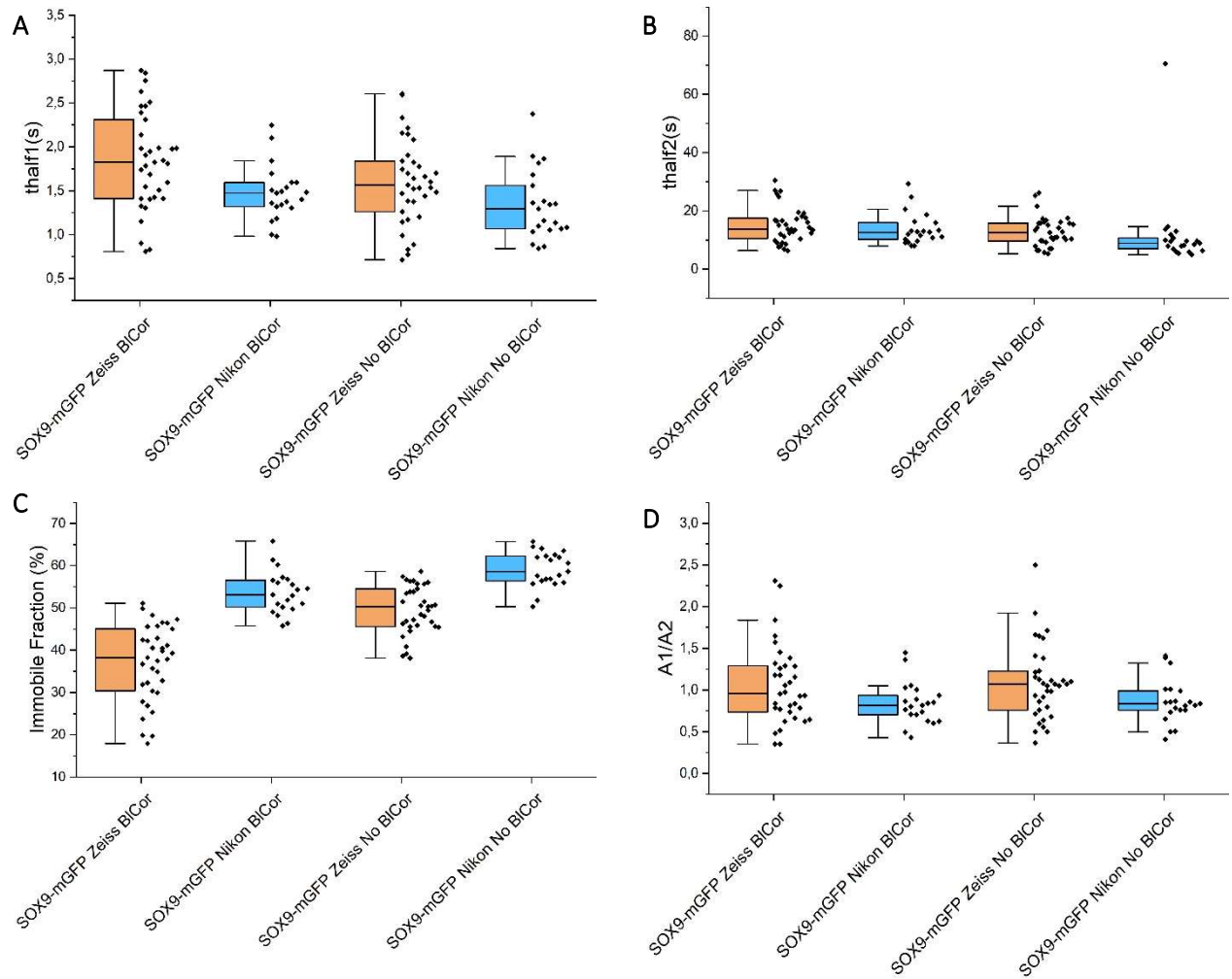


Figure 13 – Effect of BICor on the FRAP parameters of SOX9-mGFP: t_{half1} (A), t_{half2} (B), IF (C), and A_1/A_2 (D). The changes are shown for both the Zeiss and Nikon CLSM.

Appendix E – Results SOX9-mGFP + IL1 β

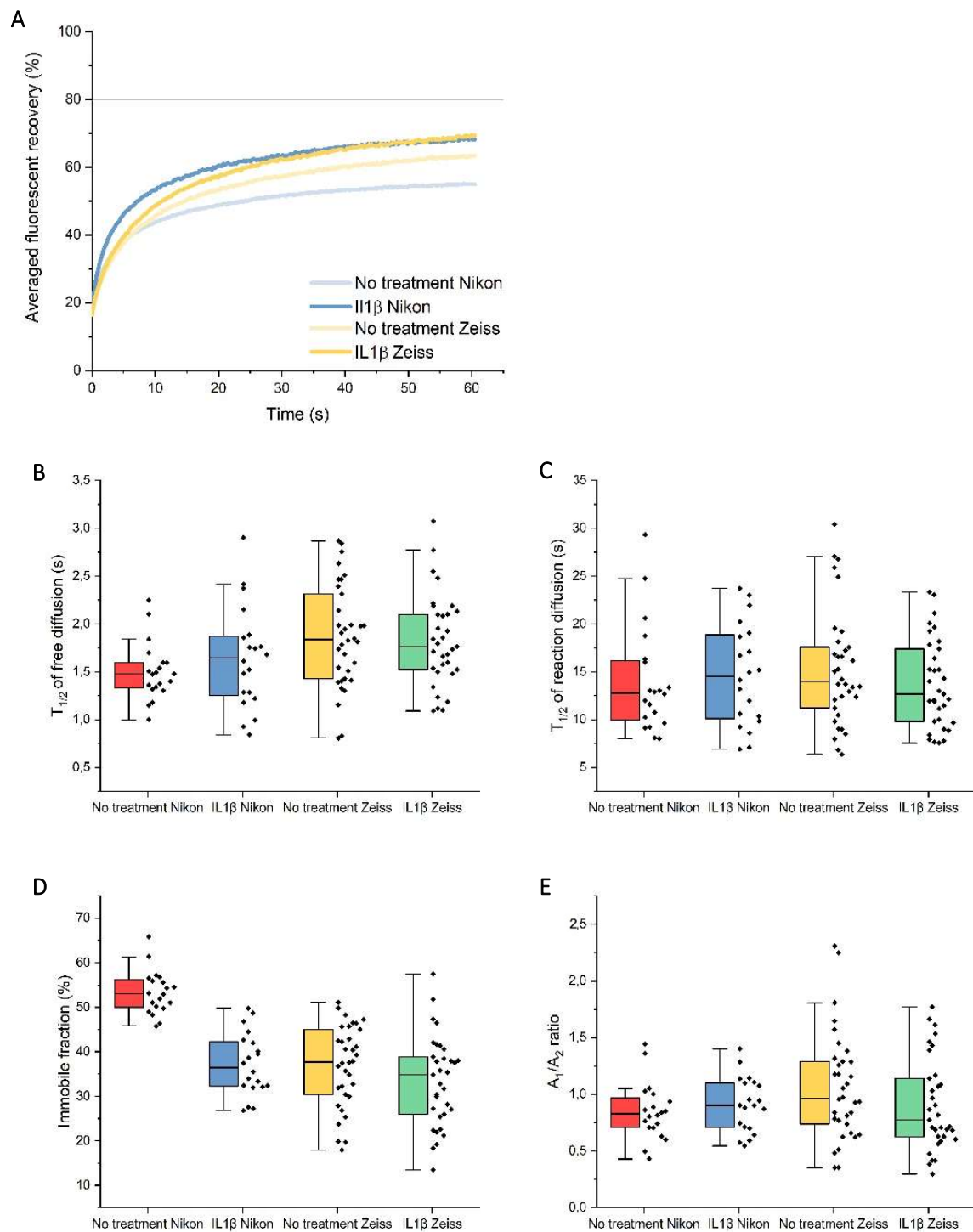


Figure 14 – (A) Recovery curves of the conditions SOX9-mGFP and SOX9-mGFP + IL1 β for the Zeiss and the Nikon. (B-E) Boxplots for the FRAP parameters t_{half1} (B), t_{half2} (C), IF (D), and A_1/A_2 (E). All values are for indicated for the conditions SOX9-mGFP and SOX9-mGFP + IL1 β for both the Zeiss and Nikon CLSM. Data is adapted from the bachelor thesis of E.S. Meima (June 2020).

Appendix F – MATLAB Script

```
1  %FrapAnalysis_txt_V1.m
2  %This script is to analyze FRAP data collected on LSM. Images are acquired
3  %and average ROI values are exported into .txt files. This script reads
4  %in the columns of numbers, subtracts background, corrects for
5  %photobleaching and then fits to exponential.
6  clear; close all; clc
7
8  datapath='C:\'; %Enter data path. Do not forget last \
9  resultspath = [datapath '\Analysis1\']; % Give name to data folder.
10 singleFit= [resultspath '\SingleFit\'];
11 doubleFit= [resultspath '\DoubleFit\'];
12 Files=dir(fullfile(datapath, '*.txt'));
13 mkdir([resultspath]);
14 mkdir([singleFit]);
15 mkdir([doubleFit]);
16
17 bleachstart=26; %time point bleaching started
18 pbcorstart=16; %time point to start the prebleach correction (may not be 1 if
19 there is weird photobleaching in the beginning)
20
21 rn=1.5877879717578075; % Bleaching spot radius. Information from Zeiss microscope
22 by ImageJ
23
24 %Effective radius measured with 'findRe.m' script and ImageJ
25 re= 3.361216667 ; % Average RE of 18 files (3 conditions)
26
27 for ii = 1:size(Files,1)
28     f=Files(ii).name;
29     %load .txt files
30     fid = fopen([datapath f], 'r');
31
32     values = textscan(fid, '%n %n %n %n %n', 'headerlines', 1);
33     fclose(fid);
34     %columns are: [time, bleachROI, bkg, correctionROI]
35     time=squeeze(double(values{2}));
36     bl=squeeze(double(values{3}));
37     bkg=squeeze(double(values{5}));
38     pb=squeeze(double(values{4}));
39
40     %subtract background, column 2
41     bl=bl-bkg;
42     pbcor=pb-bkg;
43     %Correct for photobleaching
44     blcor=bl./(pbcor./pbcor(pbcorstart)); %(can be turned off) change to start
45 calculation at time point 15 to avoid weird initial bleach for mGFP data, take 25
46 prebleach images for mGFP
47     Dimen = blcor(16:25); %takes values of last 10 time points before bleaching
48     Avg=mean(Dimen);
49     %Remove pre-bleach to start fitting after bleach
50     blcorRm=blcor(bleachstart:end);
51     timeRm=time(bleachstart:end)-time(bleachstart);
52     x=squeeze(double(timeRm));
53     y=squeeze(double(blcorRm));
54     preint=mean(blcor(pbcorstart:bleachstart-1)); %changed to start calculation at
55 time point 15 to avoid weird initial bleach when using mGFP
56     postint=blcor(bleachstart);
57     opts = fitoptions('method', 'NonlinearLeastSquares');
58
59     % Fit diffusion coefficient Curve
60     %Normalization of FRAP data by Preint (The maximum int=1)
61     ynorm=y/preint;
62     yzero=ynorm(1); %Normalized int right after photobleaching=Postint/Preint
63
64     %Bleaching depth parameter k was recalculated to match y0
65     k=(1- yzero)*(1+(rn^2/re^2));
66
```

```

67 %Nonlinear data fitting by nlinfit.m
68 % Fitting parameter 1 : p(1)=D -> Diffusion coefficient
69 % Fitting parameter 2 : p(2)=Mf -> Mobile fraction
70 t=x;
71 modelfunction = @(p,x) (1-k./(1+rn*rn/re/re+8*p(1)*t/re/re))*p(2)+(1-
72 p(2))*yzero; % Fitting function was defined
73 p= nlinfit(t, ynorm, modelfunction, [0.5 1]); % initial guess
74 k=0.5 and D=1
75
76 %Name the best fitting parameter as D and Mf
77 D=p(1);
78 Mf=p(2);
79
80 %Find the best fitting curve
81 Bf= (1-k./(1+rn*rn/re/re+8*D*t/re/re))*Mf+(1-Mf)*yzero;
82
83
84
85 %%%%%%%%%%%%%%%%%%%%%%%%%%%%%%%%%%%%%%%%%%%%%%%%%%%%%%%%%%%%%%%%%%%%%%%%%
86 % Method 2: Find D from the half time of recovery and re (effective radius)
87 thalf= findHT(t,ynorm);
88
89 D2=(re^2+rn^2)/thalf/8;
90
91
92 %%%%%%%%%%%%%%%%%%%%%%%%%%%%%%%%%%%%%%%%%%%%%%%%%%%%%%%%%%%%%%%%%%%%%%%%%
93 %Plot the best fitting curve
94 figure ;
95 plot(time-time(bleachstart),blcor/preint ,t ,Bf) ;
96 xlabel('t')
97 ylabel('f')
98 title(['D= ',num2str(D),', D_{half}= ',num2str(D2)])
99
100 %First plot and fit for single exponential
101 %opts.Upper=[y(1)*1.01,1000,100];
102 yend=y(1)*2;
103 opts.StartPoint=[y(1),yend,5];
104 opts.Lower=[y(1),1,0.1];
105 ftype =fittype('y0+A1*(1-exp(-
106 x/taul))','options',opts,'coeff',{'y0','A1','taul'},'indep','x','depen','y');
107 [results,goodness] = fit(x,y,ftype);
108 c=coeffvalues(results);
109 y0(ii,1)=c(1);
110 A1(ii,1)=c(2);
111 tau1(ii,1)=c(3);
112 thalf1(ii,1)=log(2)*c(3);
113 I0(ii,1)=preint;
114 IF(ii,1) = (1- ((A1(ii,1))/(preint-postint)))*100;
115 A2(ii,1)=0;
116 tau2(ii,1)=0;
117 thalf2(ii,1)=log(2)*0;
118
119 figure ;
120 plot(squeeze(x),squeeze(y),'bo') ;
121
122 hold on
123 plot(x,[c(1)+c(2).*(1-exp(-x./c(3)))], 'r') ;
124 xlabel(['Time (s)']);
125 ylabel('Intensity');
126 %title([f(ii)])
127 text(max(x)-10,min(y)+max(y)/20+20,['tau = ', num2str(c(3))])
128 text(max(x)-10,min(y)+20,['IF = ', num2str(IF(ii,1))])
129 title([f 'Single Fit']);
130 hold off
131
132 print(gcf, '-djpeg', [singleFit f(1:end-4) '_plot.jpg']);
133 Values= squeeze([x(:,:),y(:,:)]);
134 Nrmrlse (:,ii) =y(:,:)/Avg*100; %Normalizes to 1

```

```

135     fid = fopen([singleFit f(1:end-4) '_plotvalues.csv'],'w');
136     fprintf(fid,'%f, %f, %f \n',[Values Nrmlse(:,ii)]');
137     fclose(fid);
138     close all
139
140     % Fit diffusion coefficient Single Fit
141     %Normalization of FRAP data by Preint (The maximum int=1)
142     ySingleFit=[c(1)+c(2).*(1-exp(-x./c(3)))];
143     ynorm=ySingleFit/preint;
144     yzero=ynorm(1); %Normalized int right after photobleaching=Postint/Preint
145
146     %Bleaching depth parameter k was recalculated to match y0
147     k=(1- yzero)*(1+(rn^2/re^2));
148
149     %Nonlinear data fitting by nlinfit.m
150     % Fitting parameter 1 : p(1)=D -> Diffusion coefficient
151     % Fitting parameter 2 : p(2)=Mf -> Mobile fraction
152     t=x;
153     modelfunction = @(p,x) (1-k./(1+rn*rn/re/re+8*p(1)*t/re/re))*p(2)+(1-
154 p(2))*yzero; % Fitting function was defined
155     p= nlinfit(t, ynorm, modelfunction, [0.5 1]); % initial guess
156     k=0.5 and D=1
157
158     %Name the best fitting parameter as D and Mf
159     D1(ii,1)=p(1);
160     Mf=p(2);
161
162     %Find the best fitting curve
163     Bf1= (1-k./(1+rn*rn/re/re+8*D1(ii,1)*t/re/re))*Mf+(1-Mf)*yzero;
164
165
166
167     %%%%%%%%%%%%%%%%%%%%%%%%%%%%%%%%%%%%%%%%%%%%%%%%%%%%%%%%%%%%%%%%%%%%%%%%%
168     % Method 2: Find D from the half time of recovery and re (effective radius)
169     thalf= findHT(t,ynorm);
170
171     D2(ii,1)=(re^2+rn^2)/thalf/8;
172
173
174     %%%%%%%%%%%%%%%%%%%%%%%%%%%%%%%%%%%%%%%%%%%%%%%%%%%%%%%%%%%%%%%%%%%%%%%%%
175     %Plot the best fitting curve
176     figure ;
177     plot(time-time(bleachstart),blcor/preint ,t ,Bf1) ;
178     xlabel('t')
179     ylabel('f')
180     title(['D= ',num2str(D1(ii,1))', ' D_{half}= ',num2str(D2(ii,1))])
181     print(gcf, '-djpeg', [singleFit f(1:end-4) '_Diffusionplot.jpg']);
182
183     %Second plot and fit for two-component exponential
184     %yend=y(1)*2;
185
186     Alstart= 5500; %these are the start values for the fitting
187     A2start= 2*Alstart; %these are the start values for the fitting (A1=300,
188 A2=600)
189     tau1start=1;
190     tau2start=10;
191     opts.StartPoint=[y(1),Alstart,tau1start,A2start,tau2start]; % These values need
192 to be optimized!
193     opts.Lower=[0,1,0.1,1,1];
194     ftype = fitype('y0+A1*(1-exp(-x/tau1))+A2*(1-exp(-
195 x/tau2))','options',opts,'coeff',{'y0','A1','tau1','A2','tau2'},'indep','x','depen'
196 ,'y');
197     [results,goodness] = fit(x,y,ftype);
198     c=coeffvalues(results);
199     y0(ii,2)=c(1);
200     A1(ii,2)=c(2);
201     tau1(ii,2)=c(3);
202     thalf1(ii,2)=log(2)*c(3);

```

```

203 I0(ii,2)=preint;
204 A2(ii,2)=c(4);
205 tau2(ii,2)=c(5);
206 thalf2(ii,2)=log(2)*c(5);
207 % Calculate Immobile Fraction
208 IF(ii,2) = (1 - ((A1(ii,2)+A2(ii,2))/(I0(ii,2)-y0(ii,2))))*100;
209 Ratio (ii,2) = A1(ii,2)/A2(ii,2);
210
211 %Create Figure
212 figure ;
213 plot(squeeze(x),squeeze(y),'bo') ;
214 hold on
215 plot(x,[c(1)+c(2).*(1-exp(-x./c(3)))+c(4).*(1-exp(-x./c(5)))], 'r') ;
216 plot(x,[c(1)+c(2).*(1-exp(-x./c(3)))], 'k') ;
217 plot(x,[c(1)+c(2)+c(4).*(1-exp(-x./c(5)))], 'g') ;
218 xlabel(['Time (s)']);
219 ylabel('Intensity');
220 %title([f(ii)])
221 text(max(x)-10,min(y)+max(y)/10,['tau1= ' num2str(tau1(ii,2))])
222 text(max(x)-10,min(y)+max(y)/20,['tau2= ' num2str(tau2(ii,2))])
223 text(max(x)-10,min(y),['IF = ', num2str(IF(ii,2))])
224 title([f 'Two-Component Fit']);
225 hold off
226 %Save figure and fit values
227 print(gcf, '-djpeg', [doubleFit f(1:end-4) '_plot.jpg']);
228 Values= squeeze([x(:,:),y(:,:)]);
229
230 fid = fopen([doubleFit f(1:end-4) '_plotvalues.csv'],'w');
231 fprintf(fid,'%f, %f, %f \n',[Values Nrmlse(:,ii)]);
232 fclose(fid);
233 close all
234
235 % Fit diffusion coefficient Double Fit first part
236 %Normalization of FRAP data by Preint (The maximum int=1)
237 yDoubleFitFirst=[c(1)+c(2).*(1-exp(-x./c(3)))];
238 ynorm=yDoubleFitFirst/preint;
239 yzero=ynorm(1); %Normalized int right after photobleaching=Postint/Preint
240
241 %Bleaching depth parameter k was recalculated to match y0
242 k=(1- yzero)*(1+(rn^2/re^2));
243
244 %Nonlinear data fitting by nlinfit.m
245 % Fitting parameter 1 : p(1)=D -> Diffusion coefficient
246 % Fitting parameter 2 : p(2)=Mf -> Mobile fraction
247 t=x;
248 modelfunction = @(p,x) (1-k./(1+rn*rn/re/re+8*p(1)*t/re/re))*p(2)+(1-
249 p(2))*yzero; % Fitting function was defined
250 p= nlinfit(t, ynorm, modelfunction, [0.5 1]); % initial guess
251 k=0.5 and D=1
252
253 %Name the best fitting parameter as D and Mf
254 D11(ii,1)=p(1);
255 Mf=p(2);
256
257 %Find the best fitting curve
258 Bf11= (1-k./(1+rn*rn/re/re+8*D11(ii,1)*t/re/re))*Mf+(1-Mf)*yzero;
259
260
261
262 %%%%%%%%%%%%%%%%%%%%%%%%%%%%%%%%%%%%%%%%%%%%%%%%%%%%%%%%%%%%%%%%%%%%%%%%%
263 % Method 2: Find D from the half time of recovery and re (effective radius)
264 thalf= findHT(t,ynorm);
265
266 D21(ii,1)=(re^2+rn^2)/thalf/8;
267
268 % Fit diffusion coefficient Double Fit Second Part
269 %Normalization of FRAP data by Preint (The maximum int=1)
270 yDoubleFitSecond=[c(1)+c(2)+c(4).*(1-exp(-x./c(5)))];

```

```

271     ynorm=yDoubleFitSecond/preint;
272     yzero=ynorm(1); %Normalized int right after photobleaching=Postint/Preint
273
274     %Bleaching depth parameter k was recalculated to match y0
275     k=(1- yzero)*(1+(rn^2/re^2));
276
277     %Nonlinear data fitting by nlinfit.m
278     % Fitting parameter 1 : p(1)=D -> Diffusion coefficient
279     % Fitting parameter 2 : p(2)=Mf -> Mobile fraction
280     t=x;
281     modelfunction = @(p,x) (1-k./(1+rn*rn/re/re+8*p(1)*t/re/re))*p(2)+(1-
282 p(2))*yzero; % Fitting function was defined
283     p= nlinfit(t, ynorm, modelfunction, [0.5 1]) ; % initial guess
284     k=0.5 and D=1
285
286     %Name the best fitting parameter as D and Mf
287     D12(ii,1)=p(1);
288     Mf=p(2);
289
290     %Find the best fitting curve
291     Bf12= (1-k./(1+rn*rn/re/re+8*D12(ii,1)*t/re/re))*Mf+(1-Mf)*yzero;
292
293
294
295     %%%%%%%%%%%%%%%%%%%%%%%%%%%%%%%%%%%%%%%%%%%%%%%%%%%%%%%%%%%%%%%%%%%%%%%%%
296     % Method 2: Find D from the half time of recovery and re (effective radius)
297     thalf= findHT(t,ynorm);
298
299     D22(ii,1)=(re^2+rn^2)/thalf/8;
300
301
302     %%%%%%%%%%%%%%%%%%%%%%%%%%%%%%%%%%%%%%%%%%%%%%%%%%%%%%%%%%%%%%%%%%%%%%%%%
303     %Plot the best fitting curve
304     figure ;
305     plot(time-time(bleachstart),blcor/preint ,t ,Bf11 ,t , Bf12) ;
306     xlabel('t')
307     ylabel('f')
308     title(['D11= ',num2str(D11(ii,1))',' D11_{half}= ',num2str(D21(ii,1))',' D12=
309 ',num2str(D12(ii,1))',' D12_{half}= ',num2str(D22(ii,1))])
310     print(gcf, '-djpeg', [doubleFit f(1:end-4) '_Diffusionplot.jpg']);
311     close all
312
313 end
314
315 filename=fullfile(resultspath, 'FitResults.xls');
316 % Creates Spreadsheet with all values from both fits.
317 for ii = 1:(size(Files,1))
318     if ii==1 % don't understand but need to initiate the cell first before
319 adding in loop.
320
321 s1={'Name','y0','A1','A2','I0','tau1','tau2','thalf1','thalf2','IF','D1','D1half';
322 Files(ii).name,
323 y0(ii,1),A1(ii,1),A2(ii,1),I0(ii,1),tau1(ii,1),tau2(ii,1),thalf1(ii,1),thalf2(ii,1)
324 ,IF(ii,1),D1(ii,1),D2(ii,1)};
325
326 s2={'Name','y0','A1','A2','I0','tau1','tau2','thalf1','thalf2','IF','D11','D1half',
327 'D21','D2half','Ratio';Files(ii).name,
328 y0(ii,2),A1(ii,2),A2(ii,2),I0(ii,2),tau1(ii,2),tau2(ii,2),thalf1(ii,2),thalf2(ii,2)
329 ,IF(ii,2),D11(ii,1),D21(ii,1),D12(ii,1),D22(ii,1), Ratio(ii,2)};
330     end
331     s1(ii+1,:)={Files(ii).name,
332 y0(ii,1),A1(ii,1),A2(ii,1),I0(ii,1),tau1(ii,1),tau2(ii,1),thalf1(ii,1),thalf2(ii,1)
333 ,IF(ii,1), D1(ii,1),D2(ii,1)};
334     s2(ii+1,:)={Files(ii).name,
335 y0(ii,2),A1(ii,2),A2(ii,2),I0(ii,2),tau1(ii,2),tau2(ii,2),thalf1(ii,2),thalf2(ii,2)
336 ,IF(ii,2),D11(ii,1),D21(ii,1),D12(ii,1),D22(ii,1), Ratio(ii,2)};
337     end
338

```



```

339     xlswrite(filename, s1, 'Single Exponential Fit Values');
340     xlswrite(filename, s2, 'Two-Component Fit Values');
341
342
343 filename=fullfile(resultspath, 'FRAP.xls');
344 % Creates Spreadsheet with consolidated fit values.
345     for ii = 1:(size(Files,1))
346         Names{ii}=Files(ii).name;
347         t={'Time'};
348     end
349
350     xlswrite(filename, Names, 'FRAP', 'C1');
351     xlswrite(filename, Nrmlse, 'FRAP', 'C2');
352     xlswrite(filename, timeRm, 'FRAP', 'A2');
353     xlswrite(filename, t, 'FRAP');

```

Appendix G – Zeiss Protocol

See next page for the full protocol. The page numbers mentioned in the table of contents correspond to the page numbers in this report and not the original protocol, which is handed in separately.



FRAP PROTOCOL

Zeiss LSM 880

E.S. Meima, F. de Bree
Supervisor: Dr. Ing. J.N. Post
Daily Supervisor: Dr. K. Govindaraj
DBE Group – University of Twente
June 2021

Table of contents

1. Goals and introduction	37
1.1 Goals.....	37
1.2 Fluorescence Recovery After Photobleaching (FRAP)	37
1.3 Steps for using FRAP	39
2. Turning on microscope and PC.....	39
2.1 Hardware.....	39
2.2 Software	40
3. Locating cells	40
4. Settings FRAP experiment	41
4.1 Used FRAP settings on Zeiss	41
4.2 Loading settings.....	42
4.3 Acquisition parameter	43
4.4 Multidimensional Acquisition.....	46
5. Running experiments and gathering data	48
5.1 Starting FRAP experiment.....	48
5.2 Saving data	48
6. Turning off microscope and PC	50

1. Goals and introduction

1.1 Goals

The goal of this protocol is to inform the reader how to operate the Zeiss LSM 880 confocal microscope, set up FRAP experiments, determine optimal settings, and acquire FRAP data. This protocol can be used as a guideline for future FRAP experiments, which should make it easier for comparing obtained data.

1.2 Fluorescence Recovery After Photobleaching (FRAP)

Fluorescence Recovery After Photobleaching (FRAP) can be used to study protein dynamics in living cells. During FRAP experiments, a high-intensity laser pulse is used to bleach a (circular) region of interest (ROI). The post-bleaching fluorescence recovery in this region can be measured and plotted against time. A higher mobility will require less imaging time. ROI₁ is used for bleaching, while ROI₂ is a similar sized region placed at a location away from ROI₁ to measure the imaging-induced intensity loss. Correction for this loss is needed, because it can be assumed that this loss is present throughout the whole cell. When this loss is relatively large, the uncorrected recovery curve will show a slight decrease over time. ROI₃ is placed outside the cell and is used to measure the background intensity. The intensity for the recovery curve is normalized to the pre-bleaching intensity by subtracting the background intensity and correcting for the imaging-induced intensity loss as measured in ROI₂.

The recovery is dependent on the mobility of the protein, while the mobility is affected by two major factors: diffusion and chemical interactions. The diffusion constant (D) determines the rate of diffusion. Chemical interactions of a protein in a living cell can consist of interactions with other proteins or with DNA/RNA. Transcription factors can for example bind to DNA. The binding and dissociation constants of these interactions will affect the mobility. The protocol for FRAP is general usable, but the fitting of the FRAP curve is dependent on the complex formation and function of the protein of interest. Therefore, transcription factors need a two-component fit, instead of the general single-component fit.

Proper fitting of the FRAP curve is needed, because not all proteins have these chemical interactions. Untagged mGFP has no intracellular binding site, so the post-bleach intensity will recover almost completely seconds after photobleaching. Therefore, the recovery curve can be fitting with a so-called single-component fit. On the other hand, SOX9 can bind to DNA, so a FRAP curve of SOX9-mGFP needs a different fitting. The recovery will in this case be the result of two factors, namely fast (no or weak binding to DNA) and slow diffusion (strong binding to DNA). A single-component fit is in this case not sufficient, and a two-component fit is needed. Figure 1 shows the fittings of the recovery curves of mGFP and SOX9-mGFP. In the SOX9-mGFP recovery curve is the present of a shoulder indicated, which reveals that more than one process contributes to the post-bleach recovery. This curve also recovers slower than that of mGFP, and the recovery continues over time due to the exchange at the binding sites.

A method to gather information on TF dynamics and activity is with the use of Transcription Factor-Fluorescent Recovery After Photobleaching (TF-FRAP), which uses a two-component fit. TF-FRAP uses the principle that TFs bound the DNA are immobile, as is also mentioned above. Changes in DNA binding in response to external stimuli can also be studied with TF-FRAP.

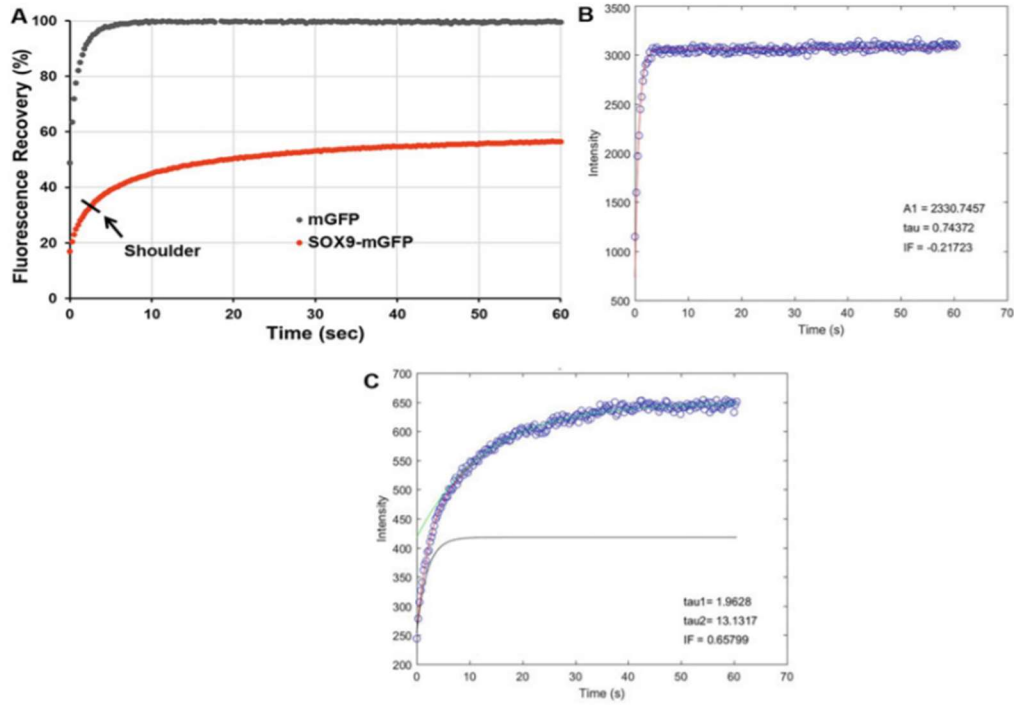


Figure 1 – (A) FRAP curves of mGFP (grey) and SOX9-mGFP (red). The SOX9-mGFP curve contains a shoulder, which is also indicated by the arrow. (B) The fitting of the mGFP curve with a single-component fit. The blue dots are data points, and the red line is the fit. (C) The SOX9-mGFP curve is fitted with a two-component fit. The blue dots are the data points. The grey and green lines are the one- and two-component fits, respectively.

Quantitative measures of protein dynamics can be derived from the TF-FRAP data, such as the immobile fraction (IF), half-time to recovery ($t_{1/2}$), and the ratio of the fast diffusing population (A_1 , unbound) to slow diffusing population (A_2 , interaction with binding site) (A_1/A_2) of the fluorescent fractions. The IF indicates the fraction of proteins that is bound to DNA, and thus immobile, and therefore will not contribute to the recovery of post-bleaching intensity. At the same time these molecules occupy binding sites for incoming unbleached proteins. The t_{half1} of A_1 and t_{half2} of A_2 indicates half the time required for the fast and slow diffusing populations to recover, respectively. A typical TF-FRAP curve fitting with a two-component fit can be seen in figure 2, together with indicated parameters.

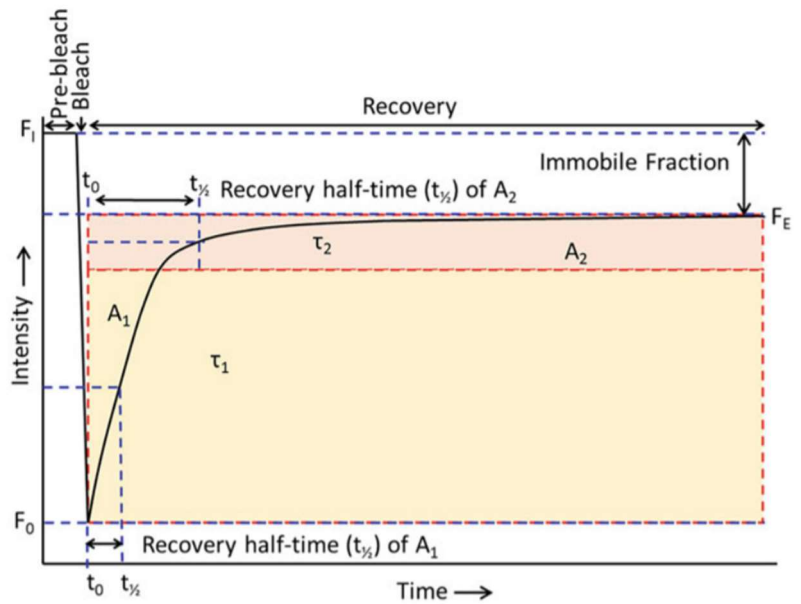


Figure 2 – Typical TF-FRAP curve. F_1 is the initial intensity, F_0 the first post-bleach intensity at t_0 , and F_E is the end intensity. $t_{1/2}$ is the half-time to recovery, which is indicated for both A_1 and A_2 . A_1 is the amplitude of the fast-diffusing population, and A_2 is the amplitude of the slow diffusing population. The immobile fraction (IF) is the difference between F_1 and F_E .

1.3 Steps for using FRAP

The protocol for FRAP can be different for each experiment, based on the cell line, fluorophore, and goal of the research, but the overall steps will be similar. These steps include:

1. Turning on microscope, PC, and software
2. Locating cells
3. Determining settings for FRAP
4. Running experiment(s)
 - a. Pre-bleach acquisition
 - b. Photobleaching
 - c. Post-bleach acquisition
5. Data saving and processing
6. Shutting down system

2. Turning on microscope and PC

2.1 Hardware

Figure 3 shows the steps for turning on the microscope and the PC. The first step is always to insert and turn the key (at the right side). After that, make sure to flip the switches in the correct order.

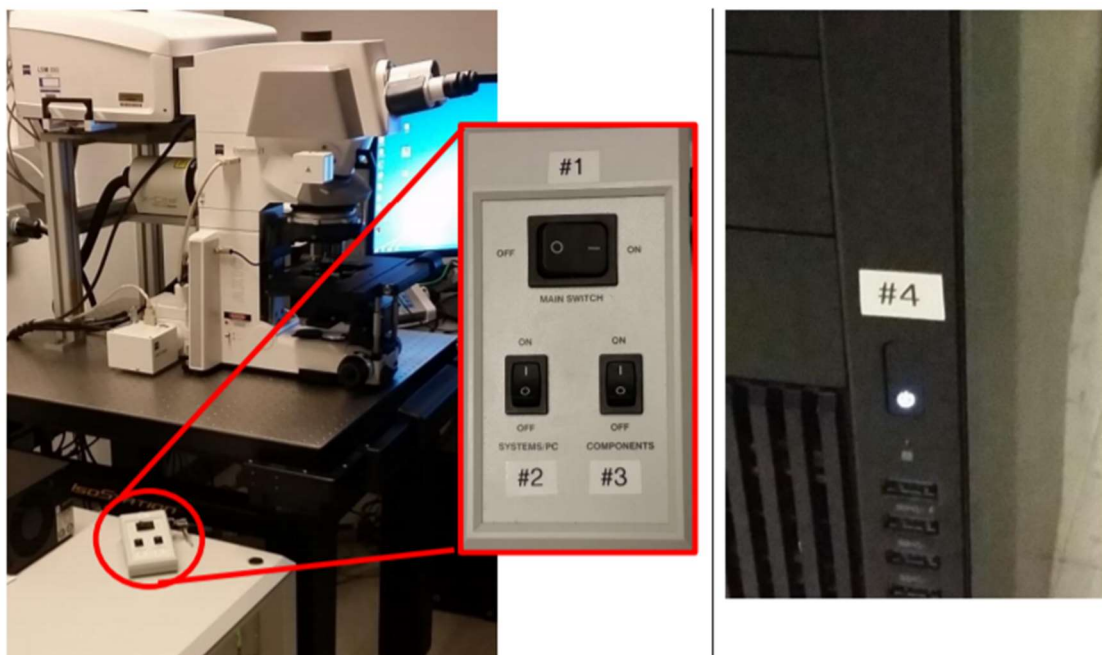


Figure 3 – Steps for turning on the microscope and the PC. The first step is always to turn on the key. After that the steps are as follows: First turn on the microscope by flipping the switches in the order shown in the picture on the left. In the PC is not already on, start the PC after the microscope is turned on.

2.2 Software

- First make sure that both the microscope and PC are turned on.
- Move the objective revolver to position 1.
- Start the software by double-clicking on the 'Zen Black' application
- Click on 'Start system', as is also shown in figure 4.



Figure 4 – Starting the Zeiss Zen software.

3. Locating cells

- Select the tab 'Locate' in the top left corner (Fig 5 A).
- The 'Microscope control' tab (Fig 5 B) shows the different elements of the microscope and allows you to change these elements via the software.
- Select the GFP reflector, turn on reflected light and make sure that the shutter is open (Fig 5 C).
- The eyepiece can now be used to locate cells and focus them.
- When a cell is focussed and in the middle of the screen, switch to the second tab: 'acquisition' (Fig 6 A).

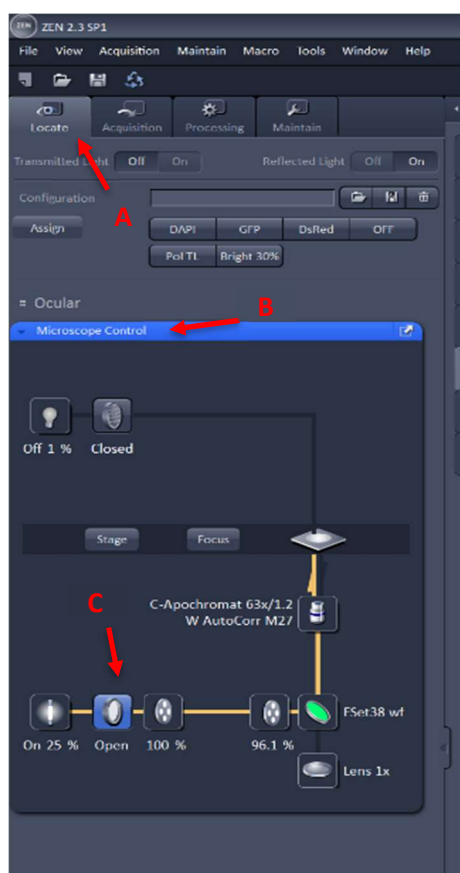


Figure 5 – Locate tab and microscope control.

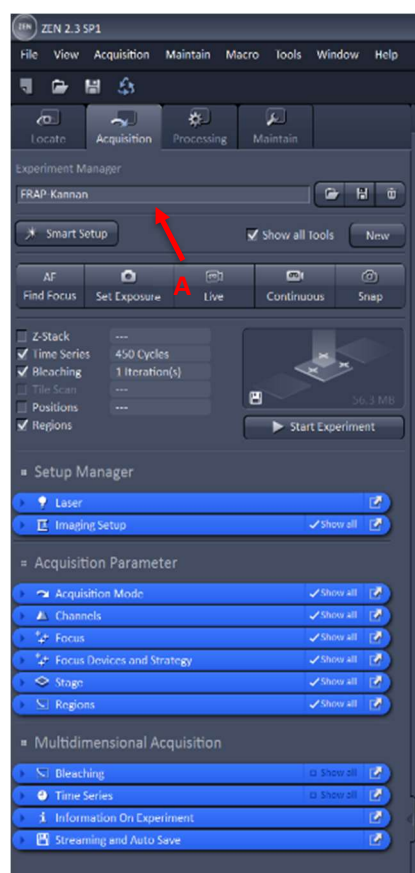


Figure 6 – Acquisition tab.

4. Settings FRAP experiment

4.1 Used FRAP settings on Zeiss

Table 1 – FRAP parameters that we have used.

Laser properties	
Objective	63x water immersion/1.2 NA
Laser	488 nm argon laser
Wavelength range	493-607 nm
Laser power	0.3%
Imaging properties	
Gain	700
Digital offset	-1
Zoom	5.0
Pinhole	1 AU (\varnothing 60 μ m)
Scanning speed	15 (this is the maximal speed for the settings used, which results in 7.7 FPS)
Frame size	256x256 pixels
Total frames	450 (\pm 1 minute)
Bleaching properties	
Pre-bleach images	25
Bleaching	1 iteration at 100% laser power
ROI-1 ROI-2 ROI-3	Width and height: 30x30 pixels (3.2 μ m)

4.2 Loading settings

- Previously saved FRAP settings can be loaded in the 'Experiment Manager'. Select the folder to the right of the bar and load for example 'FRAP Kannan' (Fig 7 A).
- Time series and bleaching will be ticked automatically by loading the settings. Regions cannot be saved. Make sure you insert these again by ticking the box 'regions' (Fig 7 B), see also section 4.3.
- Select 'show all tools' in order to see all the relevant tabs below (Fig 8 A).
- When the settings are loaded the 488nm argon laser will be used (Fig 8 B). The laser will take some time to warm up (± 5 min). During this time the laser cannot be used and will be highlighted in red in the software.
- The settings will also load the correct track for imaging fluorophores within the wavelengths of mGFP (Fig 9).
 - Note: When another fluorophore is used make sure to correct the spectrum and laser accordingly.
 - Note: A smaller spectrum can also be used in order to only detect the peak wavelength of mGFP (509 nm). You can manually adjust the range, by shifting the slider. (Fig 9 A). This is advisable when the fluorescent signal is bright enough. This way the contrast and signal-to-noise ratio will increase. This is also advisable when using multiple fluorophores.

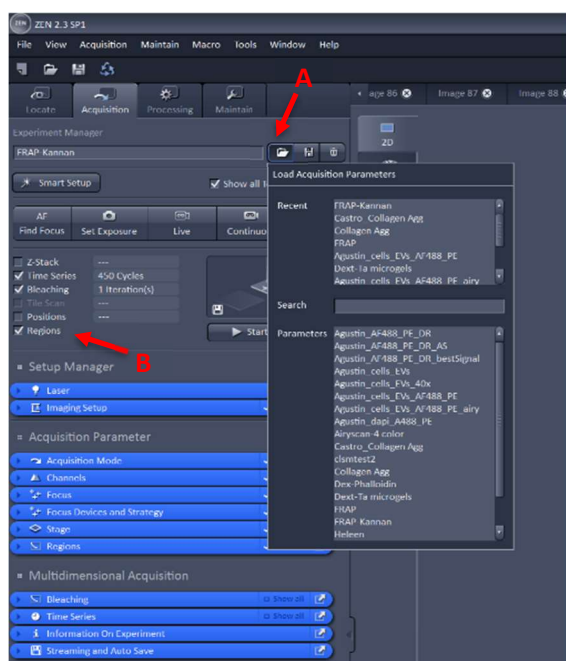


Figure 7 – Loading a previous saved setting profile.

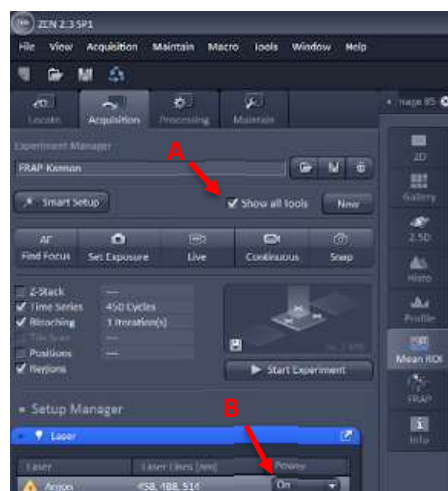


Figure 8 – Top of acquisition tab.

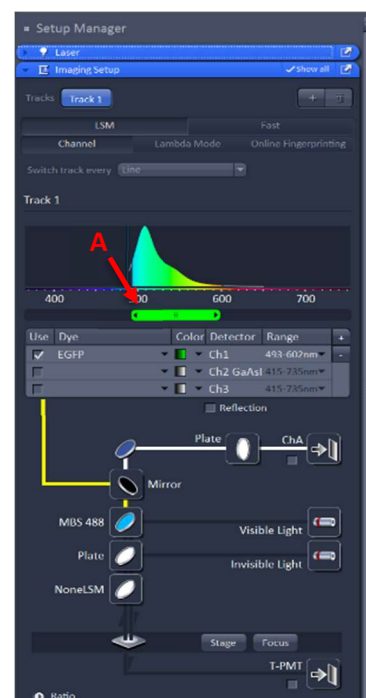


Figure 9 – GFP track.

4.3 Acquisition parameter

- The frame size, scanning speed, and zoom can be selected in the 'Acquisition mode' tab (Fig 10).
 - The frame size (Fig 10 A) used for the settings is 256x256 pixels, as is selected by loading the setting profile.
 - The scanning speed (Fig 10 B) is set to max (15), which results in a scan time of 130.25 msec (7.7 FPS).
 - The used zoom (Fig 10 C) is 5.0, which allows you to image the whole nucleus. Note that the zoom may need to be changed in order to match the imaging requirements, e.g. when imaging whole, or larger, cells. (Changing the zoom may result in a change of other parameters! Therefore it is advisable to only change the zoom when necessary.)
- The 'Channels' tab (Fig 11) shows the active tracks, used laser, intensity of the laser and gain.
 - As mentioned above, the 488 nm laser is used for GFP. The power of the laser is set to 0.3.
 - The pinhole is set to 1 AU.
 - The gain used is 700 and the digital offset was -1. This can be changed based on the average fluorescence intensity of the cells but should be kept constant during experiments in order to compare results.
 - Note: these values depend on the fluorophore used and the intensity and can therefore be different.
 - Expanding the 'display' button on the bottom of the tab will allow you to tick the 'range indicator' (Fig 11 A), which shows saturation of pixels when in live mode.

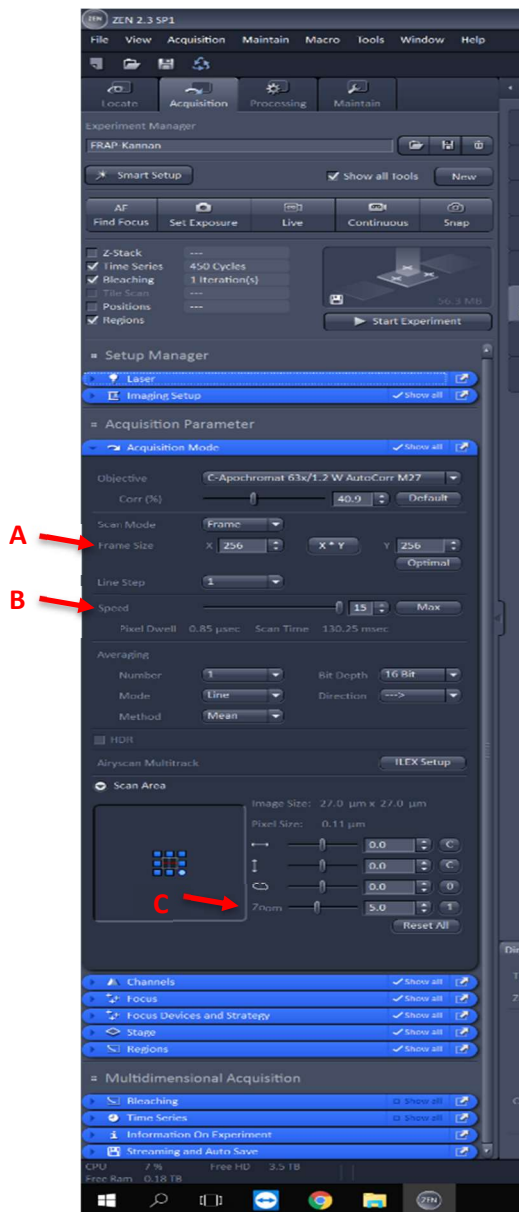


Figure 10 – Acquisition mode tab.

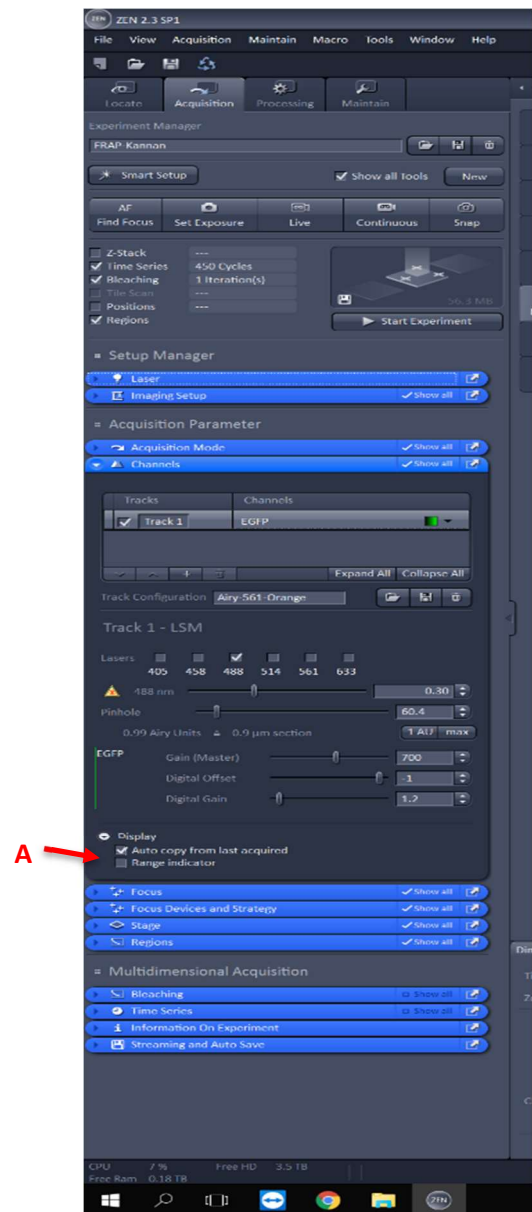


Figure 11 – Channels tab.

4.4 Multidimensional Acquisition

- The intensity and time of bleaching can be set in the 'bleaching' tab (Fig 13).
 - By ticking the first box you can set the number of frames after which the bleaching will occur. This is set to 25 (Fig 13 A).
 - The laser will bleach once (1 iteration), but this can be changed in the second line.
 - The bleaching intensity can be set at the bottom of the tab. The laser power is set to 100% (Fig 13 B).
- The 'time series' tab (Fig 14) allows you to set the total number of images.
 - The number of images should be set based on the required imaging time and the scan time (see the 'Acquisition mode' tab). The total number of images is now set to 450 (Fig 14 A). With a scanning speed of 130.25 msec the total imaging time is approximately 60 sec.

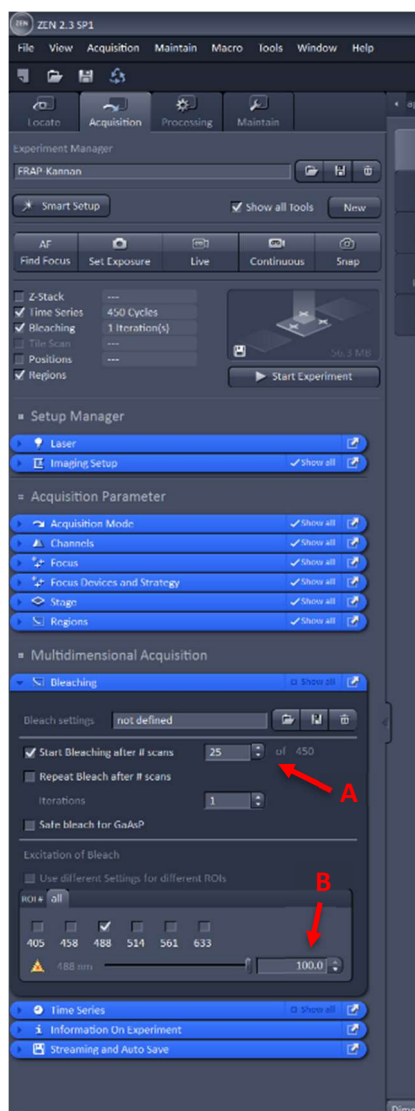


Figure 13 – The bleaching tab.

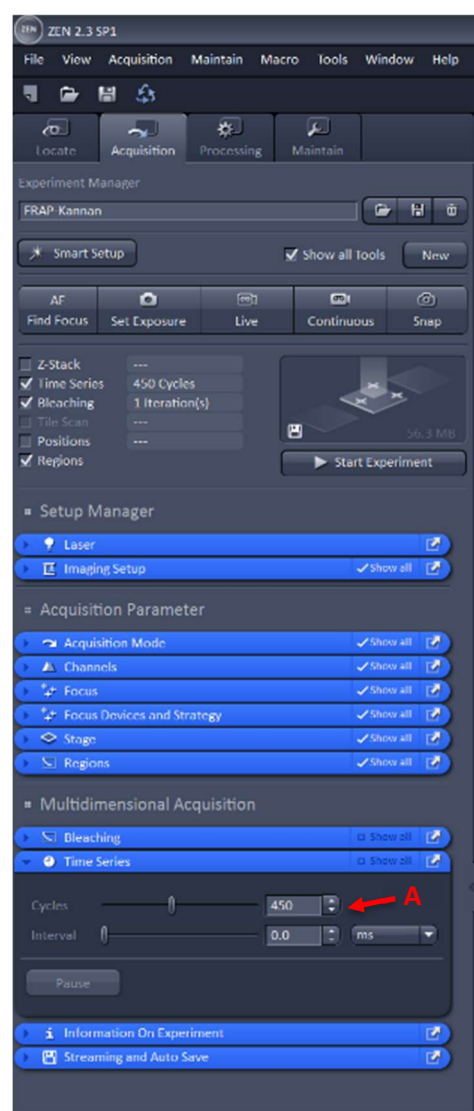


Figure 14 – The time series tab.

- The 'Streaming and Auto Save' tab (Fig 15) can be used to automatically save the data gathered with experiments.
 - Tick the 'auto save' box (Fig 15 A) and select the correct directory by clicking the three dots to the right of the bar (Fig 15 B).
 - Enter a file name for the first image. The software will automatically add the time of the experiment to the end of the filename instead of adding numbers (12_23_24 instead of 1, 2, etc.)
 - The file format can also be selected. By default this is 'Carl Zeiss Image' (.czi). These files can either be loaded into the Zen software or ImageJ/Fiji. The imaging settings can also be viewed in ImageJ and are also saved in the .czi file. An alternative is to save the data as .tif.

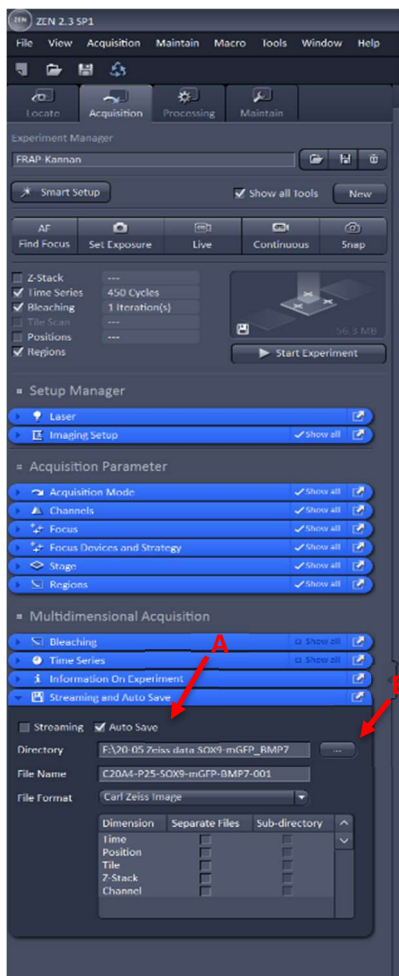


Figure 15 – The streaming and auto save tab.

5. Running experiments and gathering data

5.1 Starting FRAP experiment

- When the settings are correct and a cell is visible you can press 'Start Experiment' during live view (Fig 16 A). The experiment will run, and you can see the progress/images taken at the bar at the bottom of the screen.
- When the experiment is finished you can see the file (image) added to the workspace on the right side of the screen (Fig 16 B). You do not need to save this file manually if you have enabled auto save.
- Go to the 'FRAP' tab to the left side of the viewing screen (Fig 16 C).
 - Set each ROI to the correct function at the bottom of the tab. The red ROI is 'Group 1', the green ROI is 'Reference', and the blue ROI is 'Background' (Fig 16 D) .
 - Make sure to select the right equation (single- or two-component fit) above the ROI selection (Fig 16 E). Here you can also tick 'normalize' in order to normalize the data in the graph (Fig 16 E).
 - The graph with data point will be automatically visible, as is shown in the image below. The graph can be used to check whether drift occurs in the data or other errors are visible. The graph does not have to be saved. There is also a table below the graph which shows the calculated FRAP parameters like IF and $t_{1/2}$ (Fig 16 F).
- Next, go to the 'Mean ROI' tab, which is above the FRAP tab (Fig 17 A).
 - The intensity of the ROI's as function of time is visible in an automatically created graph. The colours of the lines correspond to the colour of the ROI's.
 - The intensity of each region on each time point is also visible in a table below the graph.
 - Note: check whether each of the regions have values in the created table. Sometimes the table is slowly generated, resulting in all zeros for a region. Check if this is the case before saving the table.

5.2 Saving data

- Right click on the table created with the intensity and time and select 'save table'. The table can be saved as a .txt file. For convenience it is advisable to save the table under the same name as the corresponding .czi file.
- Also the table with the calculated FRAP parameter values can be saved in a similar way. Go to the 'FRAP' tab, right click on the table (Fig 16 F) and select 'save table'. This table can also be saved as a .txt file.

6. Turning off microscope and PC

- Make sure your data is saved.
- Move the table upwards and remove your sample.
 - Note: if you have used the 63x objective, make sure to carefully clean the objective after usage. ONLY clean the microscope with the specific papers for the objective.
- Select a lower magnification objective by clicking on the 'objectives' tab (Fig 18 A) and then select an objective.
- You can either manually turn off the laser(s) (Fig 19 A) or do this when closing the software.
- Click 'X' in the upper right corner. The software can also ask you if you want to save files that are still open.
- A screen will appear which shows the lasers and which are still on. Here you can turn of the active lasers.
- Turn off the microscope by flipping the switched in opposite order as was indicating in Figure 3 (#3 > #2 > #1).
 - Note: the PC does not (always) have to be turned off. If you want so, you can do this before flipping the switches.
- The last step is to turn the key into the off position.

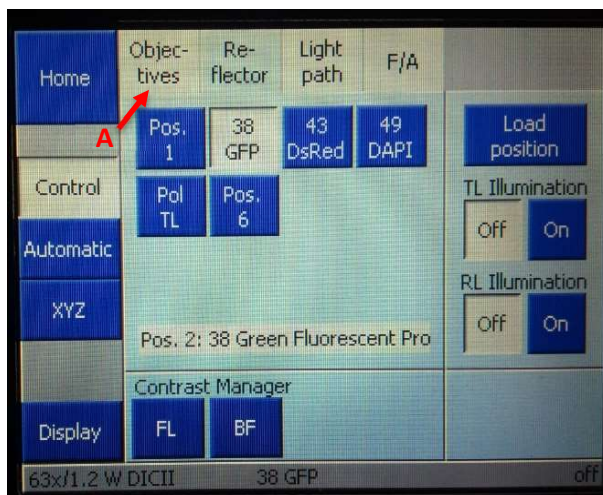


Figure 18 – Selecting the objectives tab.

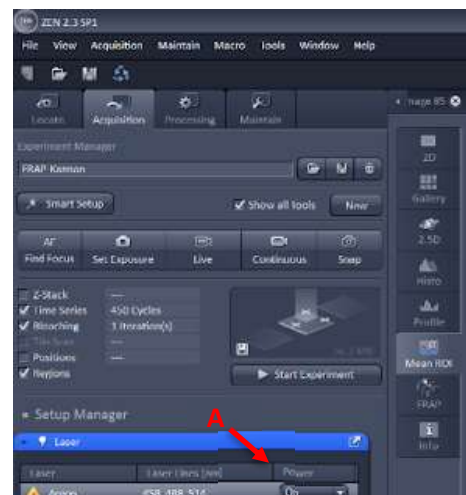


Figure 19 – Turning the laser off.